Stable and Efficient Galerkin Reduced Order Models for Non-Linear Fluid Flow

Irina Kalashnikova* and Mathew F. Barone†

Sandia National Laboratories, Albuquerque, NM 87185, U.S.A.

An efficient model reduction technique for non-linear compressible flow equations is proposed. The approach is based on the continuous Galerkin projection approach, in which the continuous governing equations are projected onto the reduced basis modes in a continuous inner product. It is an extension of the provably-stable model reduction methodology developed previously[1–3,13] for the *linearized* compressible flow equations to the *non-linear* counterparts of these equations. Attention is focussed on two challenges that arise in developing reduced order models (ROMs) for the full Navier-Stokes equations: stability and efficiency. The former challenge is addressed through the introduction of a transformation into the so-called "entropy variables". It is shown that performing the Galerkin projection step of the model reduction procedure in these variables leads to a ROM that obeys *a priori* the second law of thermodynamics, or Clausius-Duhem inequality. In this way, the ROM preserves an essential stability property of the governing equations, that of non-decreasing entropy in the solution. Although the discussion assumes that the reduced basis is constructed via the proper orthogonal decomposition (POD), the entropy stability guarantee holds for *any* choice of reduced basis, not only the POD basis. The challenge of ensuring that the model reduction technique is efficient in the presence of non-linearities is addressed using the "best points" interpolation method (BPIM) of Peraire, Nguyen *et al.*[16,17] To help gauge the viability of the proposed model reduction, some preliminary numerical studies are performed on two non-linear scalar conservation laws whose solutions possess inherently non-linear features, such as shocks and rarefactions: the Burgers equation and the Buckley-Leverett equation.

Nomenclature

ρ	= Fluid density
u_i	= Fluid velocity in the i^{th} coordinate direction, $i = 1,2,3$
δ_{ij}	= Kronecker delta ($\delta_{ij} = 1$ if $i = j$, $\delta_{ij} = 0$ otherwise)
θ	= Absolute temperature
c_v, c_p	= Specific heat at constant volume, pressure
$\imath$	= Internal energy density ($\imath = c_v\theta$)
e	= Total energy density ($e = \imath + \frac{1}{2}u_iu_i$)
γ	= Ratio of specific heats ($\gamma = c_p/c_v$)
p	= Fluid pressure ($p = (\gamma-1)\rho\imath$)
λ, μ	= Viscosity coefficients
τ_{ij}	= Viscous stress ($\tau_{ij} = \lambda u_{k,k}\delta_{ij} + \mu(u_{i,j} + u_{j,i})$)
κ	= Heat conductivity
Pr	= Prandtl number ($Pr = \mu c_p/\kappa$)
q_i	= Heat flux ($q_i = -\kappa\theta_{,i}$)
η	= Thermodynamic entropy density per unit mass
s	= Nondimensional entropy (assumed to satisfy Gibbs' equation: $s \equiv \eta/c_v = \ln(p\rho^{-\gamma}) + \text{const}$)
t	= Time
$\mathbf{x}$	= Position vector in Cartesian coordinates $\left(\mathbf{x}^T = \begin{pmatrix} x_1, & x_2, & x_3 \end{pmatrix}\right)$
$\mathbf{n}$	= Unit normal vector $\left(\mathbf{n}^T = \begin{pmatrix} n_1, & n_2, & n_3 \end{pmatrix}\right)$

*Graduate Technical Intern, Aerosciences Department, Sandia National Laboratories, P.O. Box 5800, MS 0825, Albuquerque, NM 87185 U.S.A., ikalash@sandia.gov. AIAA Member.

†Senior Member of Technical Staff, Wind Power Technologies Department, Sandia National Laboratories, P.O. Box 5800, MS 1124, Albuquerque, NM 87185 U.S.A.

Ω = Open, bounded domain
$\partial\Omega$ = Boundary of Ω
$\partial\Omega_W$ = Solid wall boundary of Ω
$\mathbf{U}$ = Vector of fluid conversation variables $\left(\mathbf{U}^T = \left(\begin{array}{cccccc} \rho, & \rho u_1, & \rho u_2, & \rho u_3, & \rho e \end{array} \right)\right)$
$\mathbf{F}_i$ = Convective (or Euler) flux in the conservation variables $\mathbf{U}$ in the i^{th} coordinate direction, $i = 1,2,3$
$\mathbf{F}_i^v$ = Viscous flux in the conservation variables $\mathbf{U}$ in the i^{th} coordinate direction, $i = 1,2,3$
$\mathbf{F}_i^h$ = Heat flux in the conservation variables $\mathbf{U}$ in the i^{th} coordinate direction, $i = 1,2,3$
$\mathbf{A}_i$ = Advective Jacobian matrices with respect to conservation variables $\mathbf{U}$, $i = 1,2,3$
$\mathbf{K}_{ij}^v$ = Viscous flux matrices in the conservation variables $\mathbf{U}$, $1 \leq i,j \leq 3$
$\mathbf{K}_{ij}^h$ = Heat flux matrices in the conservation variables $\mathbf{U}$, $1 \leq i,j \leq 3$
$\mathbf{K}_{ij}$ = Diffusivity matrices in the conservation variables $\mathbf{U}$, $1 \leq i,j \leq 3$ ($\mathbf{K}_{ij} = \mathbf{K}_{ij}^v + \mathbf{K}_{ij}^h$)
$H(\mathbf{U})$ = Generalized entropy function
$\sigma_i(\mathbf{U})$ = Entropy flux in the i^{th} coordinate direction, $i = 1,2,3$
$\mathbf{V}$ = Vector of fluid entropy variables ($\mathbf{V}^T = H_{,\mathbf{U}}$)
$\mathbf{A}_0$ = Riemannian metric tensor ($\mathbf{A}_0 = \mathbf{U}_{,\mathbf{V}}$)
$\tilde{\mathbf{F}}_i$ = Convective (or Euler) flux in the entropy variables $\mathbf{V}$ in the i^{th} coordinate direction, $i = 1,2,3$
$\tilde{\mathbf{F}}_i^v$ = Viscous flux in the entropy variables $\mathbf{V}$ in the i^{th} coordinate direction, $i = 1,2,3$
$\tilde{\mathbf{F}}_i^h$ = Heat flux in the entropy variables $\mathbf{V}$ in the i^{th} coordinate direction, $i = 1,2,3$
$\tilde{\mathbf{A}}_i$ = Advective Jacobian matrices with respect to entropy variables $\mathbf{V}$, $i = 1,2,3$
$\tilde{\mathbf{K}}_{ij}^v$ = Viscous flux matrices in the entropy variables $\mathbf{V}$, $1 \leq i,j \leq 3$
$\tilde{\mathbf{K}}_{ij}^h$ = Heat flux matrices in the entropy variables $\mathbf{V}$, $1 \leq i,j \leq 3$
$\tilde{\mathbf{K}}_{ij}$ = Diffusivity matrices in the entropy variables $\mathbf{V}$, $1 \leq i,j \leq 3$ ($\tilde{\mathbf{K}}_{ij} = \tilde{\mathbf{K}}_{ij}^v + \tilde{\mathbf{K}}_{ij}^h$)
$\tilde{\mathbf{K}}$ = Augmented diffusivity matrix in the entropy variables $\mathbf{V}$ (block (i,j) given by $\tilde{\mathbf{K}}_{ij}$, $1 \leq i,j \leq 3$)
$\mathscr{L}$ = Linear spatial differential operator
$\mathscr{N}$ = Non-linear spatial differential operator
$\mathscr{R}$ = Self-adjoint and positive semi-definite operator defining POD eigenvalue problem $\mathscr{R}\phi = \lambda\phi$
K = Number of snapshots
Δt_{snap} = Spacing between snapshots
N = Number of spatial discretization points
Δx = Spacing between spatial discretization points
M = Size of reduced basis
$\mathbf{a}_M$ = Vector of time-dependent ROM model amplitudes (coefficients) $\left(\mathbf{a}_M^T \equiv \left(\begin{array}{ccc} a_1(t), & \cdots, & a_M(t) \end{array} \right)\right)$
$\boldsymbol{\phi}_m(\mathbf{x})$ = Reduced basis modes for the fluid vector in the entropy variables $\mathbf{V}$, $m = 1,...,M$
$\mathscr{H}^M(\Omega)$ = M-dimensional POD subspace spanned by M POD modes
$\boldsymbol{\phi}_m^{\mathscr{N}}(\mathbf{x})$ = Reduced basis modes for a non-linear function $\mathscr{N}$, $m = 1,...,M$
$\boldsymbol{\psi}_m^{\mathscr{N}}(\mathbf{x})$ = Cardinal functions for a non-linear function $\mathscr{N}$, $m = 1,...,M$
$\mathbf{x}_m^{\mathscr{N}}$ = Interpolation points for a non-linear function $\mathscr{N}$, $m = 1,...,M$
$\mathbf{f}$ = Vector-valued non-linear function
$\mathscr{S}^{\mathbf{V}}$ = Set of snapshots for the entropy variables $\mathbf{V}$
$\mathscr{S}^{\mathbf{f}}$ = Set of snapshots for the non-linear function $\mathbf{f}$
$\boldsymbol{\Gamma}$ = Positive definite matrix of stabilization/shock-capturing parameters
$\mathbf{M}$ = $M \times M$ mass matrix arising in the semi-discrete ROM system with interpolation
$\mathbf{D}^{\mathbf{f}}$ = $5M \times M$ matrix arising in the semi-discrete ROM system containing the basis functions evaluated at the interpolation points for the non-linear function $\mathbf{f}$
$\mathbf{G}^{\mathbf{f}}$ = $M \times 5M$ matrix arising in the semi-discrete ROM system containing inner products of the interpolation and cardinal functions for the non-linear function $\mathbf{f}$

Subscript

i = Variable number
M = Approximation expanded in a reduced basis of order $M \in \mathbb{N}$
$,i$ = Differentiation with respect to x_i, $i = 1,2,3$ $\left(\frac{\partial}{\partial x_i}\right)$
$,t$ = Differentiation with respect to t $\left(\frac{\partial}{\partial t}\right)$
$\partial\Omega_W$ = Integration over $\partial\Omega_W$

h = High-fidelity solution

Superscript

^{T} = Matrix or vector transpose operation

$^{\text{no-slip}}$ = Application of the no-slip boundary condition

$^{\text{adiabatic}}$ = Application of the adiabatic wall boundary condition

^{bp} = "Best" interpolation points

$^{\mathscr{N}}$ = Interpolation points for the non-linear function $\mathscr{N}$

^{k} = k^{th} snapshot

I. Introduction

Despite the development of increasingly sophisticated "high-fidelity" computational fluid dynamics (CFD) tools and improved numerical methods, direct simulation of three-dimensional unsteady flow at high Reynolds and Mach numbers is in practice often too computationally expensive for use in a design or analysis setting. This situation has motivated the formulation of techniques that retain the essential physics and dynamics of a high-fidelity model, but at a much lower computational cost. The basic idea of these "Reduced Order Models" (ROMs) is to use a relatively small number of solutions generated by a high-fidelity simulation to construct a model that is much cheaper computationally, one that could be solved in real or near-real time for use in applications where simulations must be run for on-the-spot decision making, optimization, and/or control. Reduced order models can enable and enhance the understanding of complex fluid systems and non-linear dynamics in turbulent flows at a relatively low computational cost. Reduced order models are also attractive in predictive applications involving design and/or analysis, for example, flow controller design,[27] shape optimization,[28] aeroelastic stability analysis,[30,31] and the study of structural, aerodynamic and aeroelastic systems' responses to parameter variations.[32,33]

In recent years, numerous approaches to building ROMs have been proposed, each with its own inherent strengths, among them the Proper Orthogonal Decomposition (POD)/Galerkin method,[9–11] the reduced basis method,[20] balanced truncation,[21,22] and goal-oriented ROMs.[26] The use of ROMs in a predictive setting raises some fundamental questions regarding these models' numerical properties, in particular, their stability, consistency and convergence. General results for any of the three aforementioned numerical properties are lacking for POD/Galerkin models of compressible fluid flow. This leads to practical limitations of ROMs in predictive applications; for example, a ROM might be stable for a given number of modes, but unstable for other choices of basis size, as shown in Bui-Thanh *et al.*[26] and Barone, Kalashnikova *et al.*[1–3,13]

The present work is focused on techniques for building stable and efficient reduced order models for compressible flows. More specifically, a model reduction procedure based on the Proper Orthogonal Decomposition (POD)/Galerkin method is developed for the full non-linear compressible Navier-Stokes equations. These equations are required over their simpler linearized counterparts to describe satisfactorily compressible flows at transonic, supersonic and hypersonic Mach numbers, where viscous and non-linear effects (e.g., boundary layers, shocks, turbulence) are significant.

In order to be useful in predictive, real-time applications, a ROM for a non-linear set of equations, such as the formidable Navier-Stokes equations, is desired to have the following properties:

1. The ROM numerical solution should be bounded in a way that is consistent with the behavior of the exact solutions to the governing equations, i.e., the ROM should be stable.
2. The non-linear terms in the ROM should be handled in a way that does not invalidate the label *reduced* order model, i.e., the ROM should be efficient.

Although the task of developing a stable and efficient reduced order model is a particularly challenging one in the context of non-linear equations, some progress has been made in recent years.[17,23,24,28,29,36] Non-linear projection approaches for POD-based reduced order models for aerodynamics applications were investigated by LeGresley *et al.*[28] It was demonstrated by these authors that a non-linear ROM system can be solved efficiently using various least squares approximation methods. A Petrov-Galerkin method for reducing the dimension of non-linear static or dynamic computational models in real-time based on a least-squares residual minimization algorithm and the Gappy POD method[25] was proposed by Carlberg, Farhat *et al.*[24] Numerical tests revealed that this ROM can be robust, stable and accurate in difficult non-linear problems such as the prediction of turbulent flow. A POD/Galerkin ROM for the

compressible flow equations that preserves the stability of an equilibrium point at the origin has been developed by Rowley *et al.*[23] The non-linearities in the governing equations were tackled by employing an approximate, isentropic version of the equations in which only quadratic terms appeared.

In effect, this paper presents an extension of the provably-stable model reduction techniques developed previously specifically for the linearized, compressible Euler equations[1–3,13] to equations of *non-linear* and *viscous* compressible flows. As shown in these earlier works,[1–3,13] the maintenance of a proper energy balance is crucial to building a stable reduced order model. For the non-linear Euler or Navier-Stokes equations, the energy method goes hand in hand with the second law of thermodynamics, or the Clausius-Duhem inequality (Section IV), which essentially states that the entropy of a system is non-decreasing. An *a priori* entropy stability analysis (Section V) of the ROM is made possible by the fact that the proposed model reduction technique is based on the "continuous projection" approach: the continuous, governing partial differential equations (PDEs) are projected onto the reduced basis modes in a continuous inner product[1–3,13,14,20,36] (Section II). A continuous representation of the reduced basis allows the use of entropy stability analysis techniques employed in the finite element[12,37–42] and finite volume[5,8] communities to build stable numerical schemes for non-linear conservation laws, in particular the former, due to the close resemblance of the Galerkin-projected ROM equations to a finite element variational formulation. It is demonstrated that, by developing an appropriate transformation (symmetrization) of the governing equations into the so-called "entropy variables", and building the ROM in the entropy variables, it can be guaranteed that the Clausius-Duhem inequality is necessarily satisfied *ab initio* for all Galerkin ROM numerical solutions constructed for these equations. The ROM thereby preserves an essential stability property of the governing equations, that of non-decreasing entropy in the solution. This result holds for *any* reduced basis selected to represent the solution. To maintain efficiency, the second property desired of the ROM, the non-linear terms appearing in the Navier-Stokes equations are handled using the "best points interpolation method" (BPIM) proposed by Peraire, Nguyen *et. al.*[16,17] (Section III). To gauge the viability of the proposed model reduction procedure and the effectiveness of the BPIM applied to non-linear fluid equations whose solutions exhibit phenomena such as shocks and rarefactions, POD/Galerkin ROMs are constructed and evaluated numerically for two scalar non-linear conservation laws: the Burgers equation and the Buckley-Leverett equation (Section VI).

II. The POD/Galerkin Approach for Model Reduction

This section contains a brief overview of the Proper Orthogonal Decomposition (POD)/Galerkin method for reducing the order of a complex physical system governed by a general set of PDEs. The approach consists of two steps:

1. Calculation of a reduced basis using the proper orthogonal decomposition of an ensemble of flow field realizations, followed by
2. The Galerkin projection of the governing partial differential equations (PDEs) onto the reduced basis.

When successful, the result of this procedure is a set of time-dependent ordinary differential equations (ODEs) in the modal amplitudes that accurately describes the flow dynamics of the full system of PDEs for some limited set of flow conditions.

The first step in the model reduction procedure is the calculation of a reduced basis using the POD of an ensemble of realizations from a high-fidelity simulation. Discussed in detail in Lumley[15] and Holmes *et. al.*,[9] POD is a mathematical procedure that, given an ensemble of data, constructs a basis for that ensemble that is optimal in the sense that it describes more energy (on average) of the ensemble than any other linear basis of the same dimension M. In the present context, the ensemble $\{u^k(x) : k = 1,\ldots,K\}$ is a set of K instantaneous snapshots of a high fidelity numerical solution field. Mathematically, POD seeks an M-dimensional ($M << K$) subspace $\mathscr{H}^M(\Omega)$ spanned by the set $\{\phi_i\}$ such that the projection of the difference between the ensemble u^k and its projection onto $\mathscr{H}^M(\Omega)$ is minimized on average. It is a well known result[1,9,14,19] that the solution to this optimization problem reduces to the eigenvalue problem $\mathscr{R}\phi = \lambda\phi$ where $\mathscr{R} \equiv \langle u^k \otimes u^k \rangle$ is a self-adjoint and positive semi-definite operator. It can be shown[9,15] that the set of M eigenfunctions, or POD modes, $\{\phi_i : i = 1,2,\ldots,M\}$ corresponding to the M largest eigenvalues of $\mathscr{R}$ is precisely the set of $\{\phi_i\}$ that solves the aforementioned POD optimization problem. Given this basis, the numerical ROM solution u_M can be represented as a linear combination of POD modes

$$u_M(x,t) = \sum_{j=1}^{M} a_j(t)\phi_j(x), \tag{1}$$

where the $a_j(t)$ are the so-called ROM coefficients, to be solved for in the ROM.

The second step in constructing a ROM involves projecting the governing system of PDEs onto the reduced basis $\{\phi_i\}$ in some appropriate inner product, denoted generically (for now) by $(\cdot,\cdot)$. In this step, the full-system dynamics are effectively translated to the implied dynamics of the POD modes. If the governing system of equations for the state variable vector u has the form

$$\frac{\partial u}{\partial t} = \mathscr{L}u + \mathscr{N}_2(u,u) + \mathscr{N}_3(u,u,u), \tag{2}$$

where $\mathscr{L}$ is a linear differential operator, and $\mathscr{N}_2$ and $\mathscr{N}_3$ are (non-linear) quadratic and cubic operators respectively, then the Galerkin projection of (2) onto the POD mode ϕ_j for $j = 1,2,...,M$ is

$$\left(\phi_j, \frac{\partial u_M}{\partial t}\right) = (\phi_j, \mathscr{L}u_M) + (\phi_j, \mathscr{N}_2(u_M,u_M)) + (\phi_j, \mathscr{N}_3(u_M,u_M,u_M)). \tag{3}$$

Substituting the POD decomposition of u_M (1) into (3) and applying the orthonormality property of the basis functions ϕ_i in the inner product $(\cdot,\cdot)$ gives a set of time-dependent ordinary differential equations (ODEs) in the modal amplitudes (also referred to as the ROM coefficients) that accurately describes the flow dynamics of the full system of PDEs for some limited set of flow conditions:

$$\frac{da}{dt} \equiv \dot{a}_j = \sum_{l=1}^{M} a_l(\phi_j, \mathscr{L}(\phi_l)) + \sum_{l=1}^{M}\sum_{m=1}^{M} a_l a_m(\phi_j, \mathscr{N}_2(\phi_l,\phi_m)) + \sum_{l=1}^{M}\sum_{m=1}^{M}\sum_{n=1}^{M} a_l a_m a_n(\phi_j, \mathscr{N}_3(\phi_l,\phi_m,\phi_n)), \tag{4}$$

for $j = 1,2,\ldots,M$.

It is emphasized that the approach described herein is based on a Galerkin projection of the *continuous* governing partial differential equations, in common with the perspective of, for example, Barone, Kalashnikova *et al.*[1–3,13,14] This "continuous projection" approach differs from many POD/Galerkin applications, where the semi-discrete representation of the governing equations is projected, and numerical analysis proceeds from the perspective of a dynamical system of ordinary differential equations. The continuous projection approach has the advantage that the ROM solution behavior can be examined using methods that have traditionally been used for numerical analysis of spectral,[6,7] finite volume[5,8] and finite element[12,37–42] approximations to partial differential equations, such as the techniques employed herein in examining stability. Unlike in the discrete approach, however, in the continuous approach, boundary condition terms present in the discretized equation set are *not* in general inherited by the ROM.

III. Interpolation of Non-Linear Terms

The cost of forming the reduced ODE system (4) depends on the nature of the non-linearities in the original set of equations (2). Consider the general non-linear initial boundary value problem (IBVP)

$$\frac{\partial u}{\partial t} + \mathscr{L}u + \mathscr{N}(u) = f, \tag{5}$$

where $\mathscr{L}$ is a linear operator, $\mathscr{N}$ is a non-linear operator, and f is some source depending on space only (not a function of u). Projecting (5) onto the j^{th} reduced basis mode, for $j = 1,...,M$ modes gives rise to a system of ODEs of the form

$$\dot{\mathbf{a}}_M = \mathbf{F} - \mathbf{L}\mathbf{a}_M - \mathbf{N}(\mathbf{a}_M), \tag{6}$$

where $\mathbf{a}_M^T \equiv \begin{pmatrix} a_1, & \ldots & a_M \end{pmatrix}$, $L_{ij} \equiv (\mathscr{L}\phi_j, \phi_i)$, $F_i \equiv (f, \phi_i)$ for $i,j = 1,...,M$ and

$$N_i(\mathbf{a}_M) \equiv \left(\mathscr{N}\left(\sum_{k=1}^{M} a_k\phi_k\right), \phi_i\right), \qquad i = 1,...,M. \tag{7}$$

The inner products in (7) *cannot* be pre-computed prior to time-integration of the ROM system (6) if $\mathscr{N}$ contains a strong, e.g., a non-polynomial, non-linearitity. The cost of performing the required inner product is in general of $\mathscr{O}(N)$, where N is the number of spatial discretization points, which is usually quite large ($N >> M$). Hence, "direct" treatment, or computation, of these inner products can greatly reduce the efficiency of this ROM, and motivates the consideration of some alternative way to handle the non-linearity in (5).

To recover efficiency, the "best points" interpolation of Peraire, Nguyen *et al.*,[16,17] a technique based on a coefficient function approximation for the non-linear terms in (5), is employed. The general procedure is outlined in this section, and revisited in Section V.D in the context of the Navier-Stokes equations.

Suppose K snapshots have been taken of the unknown field u, at K different times (Step 1 of the POD/Galerkin approach for model reduction outlined in Section II):

$$\mathscr{S}^u \equiv \{\xi_k^u(x) = u_h^k(x) : 1 \le k \le K\}. \tag{8}$$

Given this set of snapshots of the field u, the following set of snapshots of the non-linear function $\mathscr{N}$ appearing in (5) are constructed:

$$\mathscr{S}^{\mathscr{N}} \equiv \{\xi_k^{\mathscr{N}}(x) = \mathscr{N}(u_h^k(x)) : 1 \le k \le K\}. \tag{9}$$

The best approximations of the elements in the snapshot set are now defined as

$$\mathscr{N}_M^*(u_h^k(\cdot)) = \text{argmin}_{w_M \in \text{span}\{\phi_1^{\mathscr{N}},\ldots,\phi_M^{\mathscr{N}}\}} ||\mathscr{N}(u_h^k(\cdot)) - w_M||, \qquad 1 \le k \le K, \tag{10}$$

where $\{\phi_m^{\mathscr{N}}\}_{m=1}^M$ is an orthonormal basis for $\mathscr{N}$, and $||\cdot||$ denotes the norm induced by the inner product $(\cdot,\cdot)$ in which the POD basis is constructed. Orthonormality of the $\phi_m^{\mathscr{N}}$ implies that

$$\mathscr{N}_M^*(u_h^k(x)) = \sum_{m=1}^M \alpha_m^k \phi_m^{\mathscr{N}}(x), \qquad 1 \le k \le K, \tag{11}$$

where

$$\alpha_m^k = (\phi_m^{\mathscr{N}}, \mathscr{N}(u_h^k(\cdot))), \qquad m = 1,\ldots,M, 1 \le k \le K. \tag{12}$$

The "best" interpolation points,[16,17] denoted by $\{x_m^{bp}\}_{m=1}^M$, are defined as the solution to the following optimization problem:

$$\begin{aligned} &\min_{x_1^{bp},\ldots,x_M^{bp} \in \Omega} \sum_{k=1}^K \left|\left| \mathscr{N}_M^*(u_h^k(\cdot)) - \sum_{m=1}^M \beta_m^k(x_1^{bp},\ldots,x_M^{bp})\phi_m^{\mathscr{N}} \right|\right|^2, \\ &\sum_{n=1}^M \phi_n^{\mathscr{N}}(x_m^{bp})\beta_n^k(x_1^{bp},\ldots,x_M^{bp}) = \mathscr{N}(u_h^k(x_m^{bp})), \qquad 1 \le m \le M, 1 \le k \le K, \end{aligned} \tag{13}$$

i.e., the set of points $\{x_m^{bp}\}_{m=1}^M$ is determined to minimize the average error between the interpolants $\mathscr{N}_M(\cdot)$ and the best approximations $\mathscr{N}_M^*(\cdot)$. Substituting (11) into (13) and invoking the orthonormality of the $\{\phi_m^{\mathscr{N}}\}_{m=1}^M$ gives

$$\begin{aligned} &\min_{x_1^{bp},\ldots,x_M^{bp} \in \Omega} \sum_{k=1}^K \sum_{m=1}^M (\alpha_m^k - \beta_m^k(x_1^{bp},\ldots,x_M^{bp}))^2, \\ &\sum_{n=1}^M \phi_n^{\mathscr{N}}(x_m^{bp})\beta_n^k(x_1^{bp},\ldots,x_M^{bp}) = \mathscr{N}(u_h^k(x_m^{bp})), \qquad 1 \le m \le M, 1 \le k \le K. \end{aligned} \tag{14}$$

The solution to the least-squares optimization problem (14) can be found using the Levenberg-Marquardt (LM) algorithm, and is typically reached in less than fifteen iterations of the algorithm.[17]

Given the "best points" for $\mathscr{N}$, i.e., the solutions to (14) (or any set of interpolation points), denoted by $\{x_m^{\mathscr{N}}\}_{m=1}^M$, it is straightforward to apply the interpolation procedure[16,17] to the non-linear function $\mathscr{N}(u)$ that appears in (5). The first step is to compute snapshots for the non-linear function $\mathscr{N}$ in (5). From these snapshots the interpolation points $\{x_m^{\mathscr{N}}\}_{m=1}^M$ are determined following the approach outlined above and in Section 2 of Peraire, Nguyen *et al.*[17] Given $\{x_m^{\mathscr{N}}\}_{m=1}^M$ and $\{\phi_m^{\mathscr{N}}\}_{m=1}^M$, the so-called "cardinal functions", denoted by $\{\psi_m^{\mathscr{N}}\}_{m=1}^M$, are computed by solving the following linear system[a]

$$\boldsymbol{\phi}_M^{\mathscr{N}}(x) = \mathbf{A}\boldsymbol{\psi}_M^{\mathscr{N}}(x), \tag{15}$$

where $\boldsymbol{\phi}_M^{\mathscr{N}}(x) = \left(\phi_1^{\mathscr{N}}(x),\ldots,\phi_M^{\mathscr{N}}(x)\right)^T$ and $\boldsymbol{\psi}_M^{\mathscr{N}}(x) = \left(\psi_1^{\mathscr{N}}(x),\ldots,\psi_M^{\mathscr{N}}(x)\right)^T$, and $A_{ij} = \phi_j^{\mathscr{N}}(x_i^{\mathscr{N}})$, with the cardinal functions satisfying $\psi_j(x_i^{\mathscr{N}}) = \delta_{ij}$.

Given the interpolation points $\{x_m^{\mathscr{N}}\}$ and the cardinal functions $\{\psi_m^{\mathscr{N}}\}$, the non-linear function $\mathscr{N}$ is approximated as:

$$\mathscr{N}(u) \approx \mathscr{N}_M(u) = \sum_{m=1}^M \mathscr{N}\left(u_M\left(x_m^{\mathscr{N}},t\right)\right)\psi_m^{\mathscr{N}} \in \mathbb{R}, \tag{16}$$

[a]Note that, for $\mathbf{A}$ to be invertible, the number of interpolation points must be equal to the number of modes M. A non-linear least squares optimization problem may be formulated if it is desired to have more interpolation points than modes M, but this latter approach is not considered in the present work.

so that

$$\mathscr{N}_M(u) = \sum_{m=1}^{M} \mathscr{N}\left(\sum_{n=1}^{M} a_n(t)\phi_n\left(x_m^{\mathscr{N}}\right)\right)\psi_m^{\mathscr{N}}, \tag{17}$$

where $\{\phi_m(x) : m = 1,...,M\}$ is an orthonormal basis for the solution u, computed from the snapshots (8).

The projection of $\mathscr{N}_M(u)$ onto the l^{th} POD mode for u can be written in matrix/vector form, by noting first that, for $l = 1,...,M$:

$$(\phi_l, \mathscr{N}_M(u)) = \left(\phi_l, \sum_{m=1}^{M} \mathscr{N}\left(\sum_{n=1}^{M} a_n(t)\phi_n(x_m^{\mathscr{N}})\right)\psi_m^{\mathscr{N}}\right) = \sum_{m=1}^{M}\left[\int_\Omega \phi_l \psi_m^{\mathscr{N}} d\Omega\right] \mathscr{N}\left(\sum_{n=1}^{M} a_n(t)\phi_n(x_m^{\mathscr{N}})\right). \tag{18}$$

It follows that, with the interpolation procedure employed here, the ROM ODE system for the vector of modal amplitudes $\mathbf{a}_M$ is not (6) but rather

$$\dot{\mathbf{a}}_M = \mathbf{F} - \mathbf{L}\mathbf{a}_M - \mathbf{G}^{\mathscr{N}}\mathscr{N}(\mathbf{D}^{\mathscr{N}}\mathbf{a}_M), \tag{19}$$

where $\mathbf{G}^{\mathscr{N}}$ is an $M \times M$ matrix whose entries are given by

$$G_{ij}^{\mathscr{N}} = \int_\Omega \phi_i \psi_j^{\mathscr{N}} d\Omega, \tag{20}$$

and $D_{ij}^{\mathscr{N}} = \phi_j(x_i^{\mathscr{N}})$ for $i, j = 1,...,M$.

Essentially, in the BPIM, recomputation of inner products (projection) of the non-linear terms at each time (or Newton) step is replaced by evaluation of the basis functions at the interpolation points. These interpolation points are precomputed and much fewer in number than N, the number of spatial grid points. Hence, with interpolation, the cost of each step of the online time-integration step of the model reduction procedure is of $\mathscr{O}(M)$ – compared to $\mathscr{O}(N)$ for the model reduction procedure without interpolation. Since $M << N$ in practice, the savings gained in employing the interpolation can be substantial, especially if the governing equation set possesses a strong non-linearity. The computational complexity of the "best points" interpolation algorithm is discussed in detail in Peraire, Nguyen *et al.*[16,17]

IV. Inner Product and Entropy Stability

The discussion in Sections II and III has assumed a generic inner product $(\cdot,\cdot)$, and a projection of the governing equations in the given state variables. As it turns out, the inner product employed in the Galerkin projecion step can be closely related to the numerical stability of the resulting reduced order model. This is because the inner product is a mathematical expression for the energy in the ROM. The majority of POD/Galerkin models for fluid flow use as the governing equation set the incompressible Navier-Stokes equations. Because in these models the solution vector is taken to be the velocity vector $\mathbf{u}$, so that $||\mathbf{u}||_{L^2(\Omega)}$ is a measure of the global kinetic energy in the domain Ω, the natural choice of inner product for these equations is the $L^2(\Omega)$ inner product. In effect, the $L^2(\Omega)$ inner product is physically sensible for these equations: the POD modes optimally represent the kinetic energy present in the ensemble from which they are generated. The same is *not* true for other equations arising in fluid mechanics. For example,[1–3,13] the $L^2(\Omega)$ inner product does not correspond to an energy integral for the linearized compressible Euler equations, meaning if it is selected as the inner product defining the projection, the ROM does not satisfy the energy conservation relation implied by the governing equations. For these equations, a symmetry transformation is required to yield a stable approximation. This transformation motivates the construction of a weighted $L^2(\Omega)$ inner product that guarantees certain stability bounds satisfied by the ROM solution.[1–3,13]

The aim of the present work is to employ a stability analysis akin to the stability analysis performed earlier by Barone, Kalashnikova *et al.*[1–3,13] to develop a non-linear Galerkin ROM whose numerical solution is bounded in a way consistent with behavior of exact solutions of the original non-linear differential equations, i.e. it is stable. Stability can be ensured by the energy method.[5,12] For the full (non-linear) Euler or Navier-Stokes equations, the energy method is closely tied to the second law of thermodynamics, or the Clausius-Duhem inequality, namely

$$\frac{d}{dt}\int_\Omega \rho\eta d\Omega \geq -\int_{\partial\Omega_W} \frac{q_i n_i}{\theta} dS, \tag{21}$$

where η is the thermodynamic entropy density per unit mass, ρ is the fluid density, q_i is the heat flux in the i^{th} coordinate direction, and θ is the absolute temperature. (21) essentially states that the entropy of the system is non-decreasing. For the non-linear equations of fluid mechanics, energy estimates, or the satisfaction of the entropy

inequality (21), imply that the semi-discrete solutions possess stability properties akin to those of the exact solutions of the governing equations.[5,12,42] Solutions that satisfy (21) will be referred to as "entropy stable". The aim of Section V is to develop a transformation (symmetrization) of the equations into the so-called "entropy variables" such that the Clausius-Duhem inequality (21) is necessarily satisfied for a Galerkin ROM constructed with *any* choice of reduced basis for the compressible Navier-Stokes equations in these variables.

V. An Entropy Stable and Efficient Reduced Order Model (ROM) for the 3D Compressible Navier-Stokes Equations

A. Governing Equations

In terms of the so-called conservation variables $\mathbf{U}$, the three-dimensional (3D) Navier-Stokes equations for compressible flow can be written as (neglecting forces)[12]

$$\mathbf{U}_{,t} + \mathbf{F}_{i,i} = \mathbf{F}^v_{i,i} + \mathbf{F}^h_{i,i}, \tag{22}$$

where

$$\mathbf{U} \equiv \begin{pmatrix} U_1 \\ U_2 \\ U_3 \\ U_4 \\ U_5 \end{pmatrix} \equiv \begin{pmatrix} \rho \\ \rho u_1 \\ \rho u_2 \\ \rho u_3 \\ \rho e \end{pmatrix}, \tag{23}$$

$$\mathbf{F}_i = u_i \mathbf{U} + p \begin{pmatrix} 0 \\ \delta_{1i} \\ \delta_{2i} \\ \delta_{3i} \\ u_i \end{pmatrix}, \quad \mathbf{F}^v_i = \begin{pmatrix} 0 \\ \tau_{1i} \\ \tau_{2i} \\ \tau_{3i} \\ \tau_{ij} u_j \end{pmatrix}, \quad \mathbf{F}^h_i = \begin{pmatrix} 0 \\ 0 \\ 0 \\ 0 \\ -q_i \end{pmatrix}, \tag{24}$$

for $i = 1,2,3$. $\mathbf{F}_i$ is known as the convective or Euler flux, $\mathbf{F}^v_i$ is the viscous flux, and $\mathbf{F}^h_i$ is the heat flux. The variables and parameters appearing in (23)–(24) are defined in the "Nomenclature" section of this paper. The specific heats are assumed to be positive constants. Moreover, it is required that $\mu \geq 0$, $\lambda + \frac{2}{3}\mu \geq 0$, and $\kappa \geq 0$.

(22) is the conservative form of the 3D compressible Navier-Stokes equations. These equations can also be written in non-conservative form as

$$\mathbf{U}_{,t} + \mathbf{A}_i \mathbf{U}_{,i} = (\mathbf{K}_{ij} \mathbf{U}_{,j})_{,i}, \tag{25}$$

where $\mathbf{A}_i \equiv \mathbf{A}_i(\mathbf{U})$, $\mathbf{K}^v_{ij} \equiv \mathbf{K}^v_{ij}(\mathbf{U})$ and $\mathbf{K}^h_{ij} \equiv \mathbf{K}^h_{ij}(\mathbf{U})$ are defined by

$$\mathbf{F}_{i,i} = \mathbf{F}_{i,\mathbf{U}} \mathbf{U}_{,i} \equiv \mathbf{A}_i \mathbf{U}_{,i}, \qquad \mathbf{F}^v_i \equiv \mathbf{K}^v_{ij} \mathbf{U}_{,j}, \tag{26}$$

$$\mathbf{F}^h_i \equiv \mathbf{K}^h_{ij} \mathbf{U}_{,j}, \qquad \mathbf{K}_{ij} \equiv \mathbf{K}^v_{ij} + \mathbf{K}^h_{ij}. \tag{27}$$

Neglecting for now the far-field boundary conditions, so that only the solid wall boundary conditions are considered explicitly, and denoting the solid wall boundary of the domain Ω by $\partial\Omega_W \equiv \partial\Omega$, the relevant boundary conditions to be imposed are the

$$\begin{aligned} &\text{no-slip boundary condition:} && \mathbf{u} = \mathbf{0}, && \text{on } \partial\Omega_W, \\ &\text{adiabatic wall boundary condition:} && \nabla\theta \cdot \mathbf{n} = 0, && \text{on } \partial\Omega_W. \end{aligned} \tag{28}$$

Here, θ denotes the absolute temperature. It will be assumed in the subsequent analysis that the POD (or reduced basis) modes satisfy the no-slip boundary condition (28) in the strong sense.

B. Entropy Variables for the 3D Compressible Navier-Stokes Equations

The first step to develop a Clausius-Duhem inequality preserving Galerkin projection of the equations (25) is to introduce a change of variables $\mathbf{U} \rightarrow \mathbf{V}$:

$$\mathbf{U} = \mathbf{U}(\mathbf{V}), \tag{29}$$

where $\mathbf{V}$ are the so-called "entropy variables". In terms of the entropy variables $\mathbf{V}$, the equations of interest (25) are

$$\mathbf{A}_0\mathbf{V}_{,t} + \tilde{\mathbf{A}}_i\mathbf{V}_{,i} - (\tilde{\mathbf{K}}_{ij}\mathbf{V}_{,j})_{,i} = \mathbf{0}, \tag{30}$$

where

$$\mathbf{A}_0 \equiv \mathbf{U}_{,\mathbf{V}}, \qquad \tilde{\mathbf{A}}_i \equiv \mathbf{A}_i\mathbf{A}_0, \qquad \tilde{\mathbf{K}}_{ij} \equiv \mathbf{K}_{ij}\mathbf{A}_0, \tag{31}$$

or

$$\mathbf{A}_0\mathbf{V}_{,t} + \tilde{\mathbf{F}}_{i,i}(\mathbf{V}) - (\tilde{\mathbf{K}}_{ij}\mathbf{V}_{,j})_{,i} = \mathbf{0}, \tag{32}$$

in conservative form. The entries of the matrices and vectors that appear in (30)–(32) are given in the Appendix. The Jacobian matrix $\mathbf{A}_0$ (31) plays the role of a metric tensor on $\mathbb{R}^5$, and is commonly referred to as the Riemannian metric if it is non-trivial ($\mathbf{A}_0 \neq \mathbf{I}_5$, the 5×5 identity matrix).[37,41]

It is well known that the matrices $\mathbf{A}_i$ in (25) are non-symmetric. However, it is also well known that all linear combinations of the $\mathbf{A}_i$ possess real eigenvalues and a complete set of eigenvectors, meaning that (25) constitutes a parabolic-hyperbolic system of conservation laws. The change of variables (29) is sought such that:

1. The matrices $\mathbf{A}_0$ and $\tilde{\mathbf{A}}_i$ are symmetric, and
2. The matrix

$$\tilde{\mathbf{K}} \equiv \begin{pmatrix} \tilde{\mathbf{K}}_{11} & \tilde{\mathbf{K}}_{12} & \tilde{\mathbf{K}}_{13} \\ \tilde{\mathbf{K}}_{21} & \tilde{\mathbf{K}}_{22} & \tilde{\mathbf{K}}_{23} \\ \tilde{\mathbf{K}}_{31} & \tilde{\mathbf{K}}_{32} & \tilde{\mathbf{K}}_{33} \end{pmatrix}, \tag{33}$$

   is symmetric positive semi-definite.

If there exists a transformation (29) such that these properties hold, the resulting system in the entropy variables will be symmetric parabolic if $\tilde{\mathbf{K}}$ is positive definite, and incompletely symmetric hyperbolic if $\tilde{\mathbf{K}}$ is positive semi-definite.[37]

Following previously developed symmetrization approaches,[5,12] the change of variables (29) is defined with the help of so-called generalized entropy functions. A generalized entropy function $H \equiv H(\mathbf{U})$ is by definition a function that satisfies the following two conditions:[12]

1. H is convex[b].
2. There exist scalar-valued functions $\sigma_i \equiv \sigma_i(\mathbf{U})$, $i = 1,2,3$, referred to as entropy fluxes, such that

$$H_{,\mathbf{U}}\mathbf{A}_i = \sigma_{i,\mathbf{U}}. \tag{34}$$

The following theorems[8] delineate the relationship between symmetric parabolic-hyperbolic systems and generalized entropy functions, and will be employed in the symmetrization of the equations (25).

Theorem B.1. (Mock). *A parabolic-hyperbolic system of conservation laws possessing a generalized entropy function becomes symmetric under the change of variables*

$$\mathbf{V}^T = H_{,\mathbf{U}}. \tag{35}$$

Theorem B.2. (Godunov). *If a parabolic-hyperbolic system can be symmetrized by introducing a change of variables, then a generalized entropy function and corresponding entropy fluxes exist for this system.*

[b]The convexity of H is equivalent to the positive-definiteness of $\mathbf{A}_0$, since $\mathbf{A}_0^{-1} = \mathbf{V}_{,\mathbf{U}} = H_{,\mathbf{UU}}$.

As will be shown in Theorem C.1, appropriate choices for the entropy fluxes and generalized entropy function for the compressible Navier-Stokes equations (25) are

$$\sigma_i = Hu_i, \qquad H = -\rho g(s) \equiv -\rho s, \tag{36}$$

respectively.[8,12] Here s is the non-dimensional entropy, $s = \eta/c_v$, which satisfies the well known Gibbs equation $s = \ln(p\rho^{-\gamma}) + \text{const}$.

With the choice of affine generalized entropy function (36), the transformation $\mathbf{U} \rightarrow \mathbf{V}$ (35) is given by

$$\mathbf{V} = \frac{1}{\rho_1}\begin{pmatrix} -U_5 + \rho_1(\gamma + 1 - s) \\ U_2 \\ U_3 \\ U_4 \\ -U_1 \end{pmatrix}, \tag{37}$$

where

$$s = \ln\left[\frac{(\gamma-1)\rho_1}{U_1^\gamma}\right], \qquad \rho_1 = U_5 - \frac{1}{2U_1}(U_2^2 + U_3^2 + U_4^2). \tag{38}$$

The inverse mapping $\mathbf{V} \rightarrow \mathbf{U}$ is given by

$$\mathbf{U} = \rho_1\begin{pmatrix} -V_5 \\ V_2 \\ V_3 \\ V_4 \\ 1 - \frac{1}{2V_5}(V_2^2 + V_3^2 + V_4^2) \end{pmatrix}, \tag{39}$$

where

$$\rho_1 = \left[\frac{\gamma-1}{(-V_5)^\gamma}\right]^{1/(\gamma-1)} \exp\left(\frac{-s}{\gamma-1}\right), \qquad s = \gamma - V_1 + \frac{1}{2V_5}(V_2^2 + V_3^2 + V_4^2). \tag{40}$$

Remark 1: The generalized entropy function (36) is non-unique. There exists[5] also a family of generalized entropy functions H for (30) such that $\mathbf{U}(\mathbf{V})$ and $\tilde{\mathbf{F}}(\mathbf{V})$ are both homogeneous functions of $\mathbf{V}$; that is, these functions satisfy

$$\mathbf{U}_{,\mathbf{V}}\mathbf{V} = \beta\mathbf{U}, \qquad \tilde{\mathbf{F}}_{i,\mathbf{V}}\mathbf{V} = \beta\tilde{\mathbf{F}}_i, \tag{41}$$

for some $\beta \in \mathbb{R}$. This family is known as Harten's[8] family of generalized entropy functions $H = -\rho g(s)$, e.g., the Harten exponential generalized entropy function

$$H = Ke^{\kappa s} = K(p\rho^{-\gamma}), \qquad K, \kappa \neq 0. \tag{42}$$

The generalized entropy function (42) – unlike the generalized entropy function (36) – is such that (41) holds. It can be shown that if the heat flux term $\mathbf{F}^h_{i,i}$ is present in the equations (22), the only way for the augmented heat flux matrix (33) to remain positive semi-definite is if H is affine in s, i.e., if H has the form (36). It is for this reason that the generalized entropy function (36) is selected for the compressible Navier-Stokes equations (22), instead of (42). The latter could be used for the Euler equations or the Navier-Stokes equations with $\mathbf{F}^h_{i,i} \equiv \mathbf{0}$. In the case considered here, since $\mathbf{F}^h_{i,i} \neq \mathbf{0}$, the entropy stability result in Theorem C.1 can only be obtained with the choice of affine generalized entropy function (36).

A consequence of the fact that the selected generalized entropy function does not yield the first identity in (41) is that the matrix $\mathbf{A}_0 \neq \mathbf{I}_5$ (31), making it a non-trivial Riemmanian metric. It follows that there will arise a mass matrix in the discrete ROM system to be solved for the modal amplitudes or ROM coefficients (89).

C. Entropy Stable Galerkin Projection and Weak Implementation for the Compressible Navier-Stokes Equations

The stability – namely the *ab initio* satisfaction of the Clausius–Duhem inequality – of the Galerkin projection of the symmetrized compressible Navier-Stokes equations (30) with boundary conditions (28) is now examined.

Assume the entropy variables have been expanded in a vector basis $\{\boldsymbol{\phi}_i\}_{i=1}^M \in \mathbb{R}^5$:

$$\mathbf{V}(\mathbf{x},t) \approx \mathbf{V}_M(\mathbf{x},t) = \sum_{m=1}^{M} a_m(t)\boldsymbol{\phi}_m(\mathbf{x}), \tag{43}$$

where the $a_m(t)$ are the modal amplitudes (or ROM coefficients) to be solved for, and that the basis $\{\boldsymbol{\phi}_i\}_{i=1}^M$ is orthonormal in the $L_2(\Omega)$ inner product, so that $(\boldsymbol{\phi}_i, \boldsymbol{\phi}_j) = \delta_{ij}$ for all $i, j = 1, ..., M$.

Introducing the shorthand, for $\mathbf{V}_1, \mathbf{V}_2 \in \mathbb{R}^5$,

$$(\mathbf{V}_1, \mathbf{V}_2) \equiv \int_\Omega \mathbf{V}_1^T \mathbf{V}_2 d\Omega, \qquad \langle \mathbf{V}_1, \mathbf{V}_2 \rangle_{\partial\Omega_W} \equiv \int_{\partial\Omega_W} \mathbf{V}_1^T \mathbf{V}_2 dS, \tag{44}$$

the governing equations (30) in the entropy variables projected onto a reduced basis mode $\boldsymbol{\phi}_m$, for $m = 1, ..., M$, are

$$(\boldsymbol{\phi}_m, \mathbf{A}_0 \mathbf{V}_{,t}) + \left(\boldsymbol{\phi}_m, \tilde{\mathbf{A}}_i \mathbf{V}_i\right) - \left(\boldsymbol{\phi}_m, [\tilde{\mathbf{K}}_{ij}^v \mathbf{V}_{,j}]_{,i}\right) - \left(\boldsymbol{\phi}_m, [\tilde{\mathbf{K}}_{ij}^h \mathbf{V}_{,j}]_{,i}\right) = 0. \tag{45}$$

Remark 2: From this point forward, the non-conservative form of the equations (30) will be employed, following the general approach of Hughes *et. al*[12,37,38,38–41] and Bova *et. al.*[42] In applications in which the global conservation of the advective flux is important, the second convective term in (45) should be written in "conservation form", namely

$$\left(\boldsymbol{\phi}_m, \tilde{\mathbf{A}}_i \mathbf{V}_i\right) = \left(\boldsymbol{\phi}_m, \tilde{\mathbf{F}}_{i,i}(\mathbf{V})\right) = -\left(\boldsymbol{\phi}_{m,i}, \tilde{\mathbf{F}}_i(\mathbf{V})\right) + \langle \boldsymbol{\phi}_m, \tilde{\mathbf{F}}_i(\mathbf{V}) n_i \rangle_{\partial\Omega_W}. \tag{46}$$

Although the model reduction approach developed herein is illustrated specifically on the non-conservative form of the equations (30), the extension of the formulation to the conservative equations (32) is straightforward, so there is no loss of generality in working with (30).

1. *Weak Implementation of Boundary Conditions*

In the continuous Galerkin model reduction approach, an implementation of the boundary conditions in the ROM is required. This is due to the fact that, unlike in the discrete model reduction approach, the boundary conditions present in the discretized equation set are not inherited automatically by the ROM solution. Boundary conditions are typically enforced through a weak implementation, that is, by applying them directly into the boundary integrals that arise when the governing equations are projected onto a mode, and the diffusive terms are integrated by parts.

To this effect, integration by parts of the third and fourth terms in (45) yields

$$(\boldsymbol{\phi}_m, \mathbf{A}_0 \mathbf{V}_{,t}) = -\left(\boldsymbol{\phi}_m, \tilde{\mathbf{A}}_i \mathbf{V}_i\right) - \left(\boldsymbol{\phi}_{m,i}, \tilde{\mathbf{K}}_{ij} \mathbf{V}_{,j}\right) + \underbrace{\int_{\partial\Omega_W} \boldsymbol{\phi}_m^T [\tilde{\mathbf{K}}_{ij}^v n_i \mathbf{V}_{,j}]^{\text{no-slip}} dS}_{=I_m^{\text{no slip}}} + \underbrace{\int_{\partial\Omega_W} \boldsymbol{\phi}_m^T [\tilde{\mathbf{K}}_{ij}^h n_i \mathbf{V}_{,j}]^{\text{adiabatic}} dS}_{=I_m^{\text{adiabatic}}}, \tag{47}$$

for $m = 1, ...M$. Next, the no-slip and adiabatic wall boundary conditions (28) are inserted into the boundary integrals that arise, denoted $I_m^{\text{no-slip}}$ and $I_m^{\text{adiabatic}}$ respectively. To clarify the notation, $[\mathbf{K}_{ij}^v n_i \mathbf{V}_j]^{\text{no-slip}}$ denotes the term $\mathbf{K}_{ij}^v n_i \mathbf{V}_j$ following the substitution of the no-slip boundary condition (28), and similarly for $[\mathbf{K}_{ij}^v n_i \mathbf{V}_j]^{\text{adiabatic}}$ and the adiabatic wall boundary condition. Some algebraic manipulations involving the matrices given in the Appendix reveal that

$$[\tilde{\mathbf{K}}_{ij}^v n_i \mathbf{V}_{,j}]^{\text{no-slip}} = \frac{\mu}{V_5^2} \begin{pmatrix} 0 \\ (-V_5 V_{i+1,1} + V_{i+1} V_{5,1} - V_5 V_{2,i} + V_2 V_{5,i}) n_i \\ (-V_5 V_{i+1,2} + V_{i+1} V_{5,2} - V_5 V_{3,i} + V_3 V_{5,i}) n_i \\ (-V_5 V_{i+1,3} + V_{i+1} V_{5,3} - V_5 V_{4,i} + V_4 V_{5,i}) n_i \\ 0 \end{pmatrix} + \lambda \left[\frac{-V_5 V_{i+1,i} + V_{i+1} V_{5,i}}{V_5^2} \right] \begin{pmatrix} 0 \\ n_1 \\ n_2 \\ n_3 \\ 0 \end{pmatrix}, \tag{48}$$

and

$$[\tilde{\mathbf{K}}^h_{ij} n_i \mathbf{V}_{,j}]^{\text{adiabatic}} = \mathbf{0}. \tag{49}$$

Assuming that the modes $\boldsymbol{\phi}_i$ satisfy the no-slip condition (28) in the strong sense ($\phi_i^2 = \phi_i^3 = \phi_i^4 = 0$ for $i = 1, ..., M$, where ϕ_i^j denotes the j^{th} component of $\boldsymbol{\phi}_i$), it is straightforward to see from (48) that

$$I_m^{\text{no-slip}} = 0, \tag{50}$$

for all m (since $\boldsymbol{\phi}_m^T [\tilde{\mathbf{K}}^v_{ij} n_i \mathbf{V}_{,j}]^{\text{no-slip}} = 0$). Similarly, from (49),

$$I_m^{\text{adiabatic}} = 0, \tag{51}$$

for all m. Hence, the weak form of the problem with a weak implementation of the relevant boundary conditions (28) is simply

$$(\boldsymbol{\phi}_m, \mathbf{A}_0 \mathbf{V}_{,t}) = -\left(\boldsymbol{\phi}_m, \tilde{\mathbf{A}}_i \mathbf{V}_i\right) - \left(\boldsymbol{\phi}_{m,i}, \tilde{\mathbf{K}}_{ij} \mathbf{V}_{,j}\right). \tag{52}$$

2. *Entropy Stability of the Galerkin-Projected Compressible Navier-Stokes Equations with Boundary Conditions*

The Galerkin projection is termed "entropy stable" if it satisfies the Clausius-Duhem entropy inequality (21), a statement of the second law of thermodynamics. It is shown in Theorem C.1 that the change of variables (37) is such that when the transformed equations (30) are projected onto a reduced basis mode and the boundary conditions (28) are applied through a weak formulation, the Clausius-Duhem inequality is respected *ab initio* for all numerical solutions.

Theorem C.1. *Consider the symmetrized compressible 3D Navier-Stokes equations* (30) *in an open bounded domain* $\Omega \subset \mathbb{R}^3$*, with the no-slip and adiabatic wall boundary condition* (28) *on the boundary* $\partial\Omega_W$*. Define the transformation* $\mathbf{U} \to \mathbf{V}$ *given by* (35) *with the affine generalized entropy function* (36)*, so that the relationship between the conservation variables* $\mathbf{U}$ *and the entropy variables* $\mathbf{V}$ *is* (37)*. Assume the modes* $\boldsymbol{\phi}_j$ *satisfy the no-slip condition on* $\partial\Omega_W$*. Then the Galerkin projection of* (30) *with boundary conditions* (28) *in the* $L^2(\Omega)$ *inner product is "entropy stable", with entropy estimate*

$$\frac{d}{dt} \int_\Omega \rho \eta \, d\Omega \geq 0. \tag{53}$$

Proof. Premultiplying (30) by $\mathbf{V}^T$ and integrating over Ω gives

$$\int_\Omega \mathbf{V}^T \mathbf{A}_0 \mathbf{V}_{,t} d\Omega + \int_\Omega \mathbf{V}^T \tilde{\mathbf{A}}_i \mathbf{V}_{,i} d\Omega - \int_\Omega \mathbf{V}^T (\tilde{\mathbf{K}}_{ij} \mathbf{V}_{,j})_{,i} d\Omega = 0. \tag{54}$$

Expanding the first term in (54),

$$\int_\Omega \mathbf{V}^T \mathbf{A}_0 \mathbf{V}_{,t} d\Omega = \int_\Omega H_{,\mathbf{U}} \mathbf{U}_{,\mathbf{V}} \mathbf{V}_{,t} d\Omega = \int_\Omega H_{,\mathbf{U}} \mathbf{U}_{,t} d\Omega = \int_\Omega H_{,t} d\Omega. \tag{55}$$

Note that

$$\mathbf{V}^T \tilde{\mathbf{A}}_i = (H_{,\mathbf{U}} \mathbf{A}_i) \mathbf{A}_0 = \sigma_{i,\mathbf{U}} \mathbf{U}_{,\mathbf{V}} = \sigma_{i,\mathbf{V}}, \tag{56}$$

so that the convection term in (54) becomes

$$\int_\Omega \mathbf{V}^T \tilde{\mathbf{A}}_i \mathbf{V}_{,i} d\Omega = \int_\Omega \underbrace{\sigma_{i,\mathbf{V}} \mathbf{V}_{,i}}_{\sigma_{i,i}} d\Omega = \int_\Omega (H u_i)_{,i} d\Omega. \tag{57}$$

Now, the diffusive term in (54) simplifies as follows:

$$\begin{aligned}
\textstyle\int_\Omega \mathbf{V}^T (\tilde{\mathbf{K}}_{ij} \mathbf{V}_{,j})_{,i} d\Omega \quad &= -\textstyle\int_\Omega \mathbf{V}^T_{,i} \tilde{\mathbf{K}}_{ij} \mathbf{V}_{,j} d\Omega + \int_{\partial\Omega_W} \mathbf{V}^T \tilde{\mathbf{K}}_{ij} n_i \mathbf{V}_{,j} dS \\
&= -\textstyle\int_\Omega \mathbf{V}^T_{,i} \tilde{\mathbf{K}}_{ij} \mathbf{V}_{,j} d\Omega + \int_{\partial\Omega_W} \mathbf{V}^T \mathbf{K}_{ij} n_i \mathbf{A}_0 \mathbf{V}_{,j} dS \\
&= -\textstyle\int_\Omega \mathbf{V}^T_{,i} \tilde{\mathbf{K}}_{ij} \mathbf{V}_{,j} d\Omega + \int_{\partial\Omega_W} \mathbf{V}^T (\mathbf{K}^v_{ij} + \mathbf{K}^h_{ij}) n_i \mathbf{U}_{,\mathbf{V}} \mathbf{V}_{,j} dS \\
&= -\textstyle\int_\Omega \mathbf{V}^T_{,i} \tilde{\mathbf{K}}_{ij} \mathbf{V}_{,j} d\Omega + \int_{\partial\Omega_W} \mathbf{V}^T (\mathbf{K}^v_{ij} + \mathbf{K}^h_{ij}) n_i \mathbf{U}_{,j} dS \\
&= -\textstyle\int_\Omega \mathbf{V}^T_{,i} \tilde{\mathbf{K}}_{ij} \mathbf{V}_{,j} d\Omega + \int_{\partial\Omega_W} \mathbf{V}^T (\mathbf{F}^v_i + \mathbf{F}^h_i) n_i dS \\
&= -\textstyle\int_\Omega \mathbf{V}^T_{,i} \tilde{\mathbf{K}}_{ij} \mathbf{V}_{,j} d\Omega + \int_{\partial\Omega_W} \mathbf{V}^T \mathbf{F}^v_i n_i dS + \frac{1}{c_v} \int_{\partial\Omega_W} \frac{q_i n_i}{\theta} dS.
\end{aligned} \tag{58}$$

Some algebraic manipulations of the $\tilde{\mathbf{K}}_{ij}$ matrices given in the Appendix reveal that the expression for $[\mathbf{F}_i^v n_i]^{\text{no-slip}}$ is (48), where $[\mathbf{F}_i^v n_i]^{\text{no-slip}}$ denotes the term $\mathbf{F}_i^v n_i$ following the substitution of the no-slip boundary condition (28). Let $\boldsymbol{\phi}_j \in \mathbb{R}^5$ be a reduced basis mode for the unknown field in the entropy variables approximated as a linear combination of the reduced basis modes, that is by $\mathbf{V}(\mathbf{x},t) \approx \sum_{m=1}^{M} a_m(t)\boldsymbol{\phi}_m(\mathbf{x})$, and assume that $\boldsymbol{\phi}_j$ satisfies the no-slip condition. Then, it follows from (48) that $[\boldsymbol{\phi}_j^T \mathbf{F}_i^v n_i]^{\text{no-slip}} = 0$ necessarily for all j, meaning $[\mathbf{V}^T \mathbf{F}_i^v n_i]^{\text{no-slip}} = 0$.

Combining (55), (57) and (58) gives the following bound

$$\begin{aligned}
\tfrac{1}{c_v}\textstyle\int_\Omega (\rho\eta)_{,t} d\Omega &= \textstyle\int_\Omega \mathbf{V}_{,i}^T \tilde{\mathbf{K}}_{ij} \mathbf{V}_{,j} d\Omega + \int_\Omega \left[-(Hu_i)_{,i} - \tfrac{1}{c_v}\left(\tfrac{q_i}{\theta}\right)_{,i} \right] d\Omega \\
&= \textstyle\int_\Omega \mathbf{V}_{,i}^T \tilde{\mathbf{K}}_{ij} \mathbf{V}_{,j} d\Omega + \int_{\partial\Omega_W} \left[-H \underbrace{u_i n_i}_{=0 \text{ (by no-slip BC)}} - \underbrace{\frac{1}{c_v}\left(\frac{q_i}{\theta}\right) n_i}_{=0 \text{ (by adiabatic wall BC)}} \right] dS \\
&= \textstyle\int_\Omega \nabla\mathbf{V}^T \tilde{\mathbf{K}} \nabla\mathbf{V} d\Omega \\
&\geq 0,
\end{aligned} \tag{59}$$

by the positive semi-definiteness of the matrix $\tilde{\mathbf{K}}$ (33), where $\nabla\mathbf{V}^T \equiv \begin{pmatrix} \mathbf{V}_{,1}, & \mathbf{V}_{,2}, & \mathbf{V}_{,3} \end{pmatrix}$. Hence,

$$\frac{d}{dt}\int_\Omega \rho\eta \, d\Omega \geq 0, \tag{60}$$

which implies non-decreasing entropy (21), and therefore entropy stability of the Galerkin projection. □

The practical consequence of Theorem C.1 is that the numerical solution always satisfies the Clausius-Duhem inequality for *any* choice of reduced basis. The continuous representation of the reduced basis is what enables the proof of this result.

3. Stabilization and Shock-Capturing

It is well known[12] that the standard Galerkin method can be ineffective when applied to flows that contain sharp boundary layers, internal layers and/or shocks: typically the computed solution exhibits spurious localized oscillations in the vicinity of a layer or a shock. To remedy this difficulty, a common approach taken by the finite element community[12,37–42] is to add to the right hand side of the weak form (54) a weighted residual term of the form

$$\left(\mathbf{A}_0\mathbf{V}_{,t} - \tilde{\mathbf{A}}_i\mathbf{V}_{,i} + (\tilde{\mathbf{K}}_{ij}\mathbf{V}_{,j})_{,i}, \boldsymbol{\Gamma}(\mathbf{A}_0\mathbf{V}_{,t} - \tilde{\mathbf{A}}_i\mathbf{V}_{,i} + (\tilde{\mathbf{K}}_{ij}\mathbf{V}_{,j})_{,i})\right), \tag{61}$$

where $\boldsymbol{\Gamma}$ is a positive-definite matrix of stabilization and/or discontinuity-capturing parameters whose entries are specified to suppress spurious oscillations in the presense of sharp layers and/or shocks.[39] Although the development of these terms is beyond the scope of the present work, it is noted that the result of Theorem C.1 still holds if stabilization terms resembling (61) are added to the equation (52), since

$$\left(\mathbf{A}_0\mathbf{V}_{,t} - \tilde{\mathbf{A}}_i\mathbf{V}_{,i} + (\tilde{\mathbf{K}}_{ij}\mathbf{V}_{,j})_{,i}, \boldsymbol{\Gamma}(\mathbf{A}_0\mathbf{V}_{,t} - \tilde{\mathbf{A}}_i\mathbf{V}_{,i} + (\tilde{\mathbf{K}}_{ij}\mathbf{V}_{,j})_{,i})\right) \geq 0, \tag{62}$$

provided $\boldsymbol{\Gamma}$ is positive definite.

D. Interpolation and Discretization

Having established *a priori* the entropy stability of the weak formulation following the Galerkin projection and boundary condition application steps of the proposed model reduction procedure (52), the next step is to discretize this weak form.

Substituting the modal expansion (43) into (52), gives, for $m = 1, \ldots, M$,

$$\sum_{n=1}^{M} (\boldsymbol{\phi}_m, [\mathbf{A}_0]_M \boldsymbol{\phi}_n)\, \dot{a}_n = -\left(\boldsymbol{\phi}_m, [\tilde{\mathbf{A}}_i]_M \mathbf{V}_{M,i}\right) - (\boldsymbol{\phi}_{m,i}, [\tilde{\mathbf{K}}_{ij}]_M \mathbf{V}_{M,j}), \tag{63}$$

where $[\mathbf{A}_0]_M \equiv \mathbf{A}_0(\mathbf{V}_M) = \mathbf{A}_0\left(\sum_{n=1}^{M} a_n(t)\boldsymbol{\phi}_n(\mathbf{x})\right)$ and similarly for the other matrices with "M" subscripts in (63).

All the terms in the projected equations (63) contain non-linearities, including the term on the left hand side. These non-linear terms will be denoted as follows:

$$[\mathbf{f}_0(\mathbf{V}_M)]_n = [\mathbf{A}_0]_M \boldsymbol{\phi}_n, \qquad n = 1,...,M, \tag{64}$$

$$\mathbf{f}_1(\mathbf{V}_M) \equiv [\tilde{\mathbf{A}}_i]_M \mathbf{V}_{M,i}, \tag{65}$$

and

$$\mathbf{f}_{i+1}(\mathbf{V}_M) \equiv [\tilde{\mathbf{K}}_{ij}]_M \mathbf{V}_{M,j}, \qquad i = 1,2,3, \tag{66}$$

where

$$\mathbf{f}_i(\mathbf{V}_M) \equiv \mathbf{f}_i\left(\sum_{m=1}^{M} a_m(t)\boldsymbol{\phi}_m(\mathbf{x})\right), \qquad i = 0,...,4. \tag{67}$$

In this notation, (63) has the form

$$\sum_{n=1}^{M} (\boldsymbol{\phi}_m, [\mathbf{f}_0(\mathbf{V}_M)]_n)\,\dot{a}_n = -(\boldsymbol{\phi}_m, \mathbf{f}_1(\mathbf{V}_M)) - \sum_{i=1}^{3} (\boldsymbol{\phi}_{m,i}, \mathbf{f}_{i+1}(\mathbf{V}_M)), \tag{68}$$

for $m = 1,...,M$. Once discretized in time, (68) will yield a non-linear discrete system of equations to be advanced in time (given an initial condition $\mathbf{V}(0,\mathbf{x}) = \mathbf{V}_0(\mathbf{x})$) using an explicit time integration scheme, or an implicit scheme combined with Newton's method at each time step. Note that the left hand side of (68) will give rise to a mass matrix that would need to be factorized during the time-integration of the ROM. This is a consequence of the fact the fact that the chosen affine generalized entropy function (36) is such that $\mathbf{U}(\mathbf{V})$ is not homogeneous in $\mathbf{V}$ (Remark 1).

1. *Semi-Discrete ROM System Following Interpolation*

The functions $\mathbf{f}_i$ (64)–(66) are highly non-linear in the entries of $\mathbf{V}$. Thus, direct treatment of the terms involving inner products with these functions would invalidate the term *reduced* order model: these inner products would need to be re-computed in each time (or Newton) step, which would have a cost depending on N, the (typically large) number of spatial discretization points. To recover efficiency, the coefficient function approximation to the non-linear terms in this expression described in Section III is applied to the system (68).

Per the discussion in Section III, the first step is to compute K snapshots of the entropy variable field $\mathbf{V}$ from a high-fidelity solution, at K different times t_k:

$$\mathscr{S}^{\mathbf{V}} \equiv \{\boldsymbol{\xi}_k^{\mathbf{V}}(\mathbf{x}) = \mathbf{V}_h^k(\mathbf{x}) : 1 \le k \le K\}. \tag{69}$$

Given this set of snapshots of the flow field, snapshots for each of the non-linear functions in (64) – (66) are computed:

$$\mathscr{S}^{[\mathbf{f}_0]_n} \equiv \{\boldsymbol{\xi}_k^{[\mathbf{f}_0]_n}(\mathbf{x}) = [\mathbf{f}_0(\mathbf{V}_h^k(\mathbf{x}))]_n : 1 \le k \le K\}, \qquad n = 1,...,M, \tag{70}$$

$$\mathscr{S}^{\mathbf{f}_j} \equiv \{\boldsymbol{\xi}_k^{\mathbf{f}_j}(\mathbf{x}) = \mathbf{f}_j(\mathbf{V}_h^k(\mathbf{x})) : 1 \le k \le K\}, \qquad j = 1,...,4. \tag{71}$$

The "best" (or any) interpolation points for each of the non-linear functions (64)–(66) will be denoted by

$$\left\{\mathbf{x}_m^{[\mathbf{f}_0]_n}\right\}_{m=1}^{M}: \quad \text{"best" (or any) interpolation points for } [\mathbf{f}_0]_n, n = 1,...,M, \tag{72}$$

$$\left\{\mathbf{x}_m^{\mathbf{f}_j}\right\}_{m=1}^{M}: \quad \text{"best" (or any) interpolation points for } \mathbf{f}_j, j = 1,...,4. \tag{73}$$

The main difference between the non-linear functions that appear in the projected Navier-Stokes equations (68) and the model problem considered in Section III is that the non-linear functions in the former are vector-valued. However, in practice, this poses no difficulty for the solution procedure of Section III: this exact procedure can be applied to each *component* of each of the non-linear vector-valued function in (64)–(66). For concreteness, and without loss of generality, let $\mathbf{f}_j \in \mathbb{R}^5$ be any of the vector-valued functions in (64)–(66), and let f_j^i denote the i^{th} component of $\mathbf{f}_j$ for $j = 0...,4$, $i = 1,...,5$. Then, each of the components of each of the functions $\mathbf{f}_j$ can be expanded in an orthonormal

(scalar) basis as, denoted here by $\left\{\phi_m^{f_j^i}\right\}_{m=1}^M$. The best approximations of the elements in the snapshot set are defined as

$$[f_j^i]_M^*(\mathbf{V}_h^k) = \sum_{m=1}^M \alpha_m^{f_j^i} \phi_m^{f_j^i}(\mathbf{x}), \qquad 1 \le k \le K, \tag{74}$$

where

$$\alpha_m^{f_j^i} = (\phi_m, f_j^i(\mathbf{V}_h^k(\cdot))), \qquad m = 1,...,M, 1 \le k \le K, \tag{75}$$

for $i = 1,...,5$, $j = 0,...,4$. Now, the interpolation points for each component of each non-linear function $\left\{\mathbf{x}_m^{f_j^i}\right\}_{m=1}^M \in \Omega \subset \mathbb{R}^3$ are defined as the solution to the following optimization problem:

$$\begin{aligned} &\min_{\mathbf{x}_1,...,\mathbf{x}_M \in \Omega} \left|\left| [f_j^i]_M^*(\cdot) - \textstyle\sum_{m=1}^M \beta_m^{f_j^i}(\mathbf{x}_1,...,\mathbf{x}_M)\phi_m^{f_j^i} \right|\right|^2 \\ &\textstyle\sum_{n=1}^M \phi_n^{f_j^i}(\mathbf{x}_m)\beta_n^{f_j^i}(\mathbf{x}_1,...,\mathbf{x}_M) = f_j^i(\mathbf{x}_m), \qquad 1 \le m \le M, \end{aligned} \tag{76}$$

so that the set of points $\left\{\mathbf{x}_m^{f_j^i}\right\}_{m=1}^M$ is determined to minimize the average error between the interpolants $[f_j^i]_M(\cdot)$ and the best approximations $[f_j^i]_M^*(\cdot)$. Substituting (74) into (76) and invoking the orthonormality of the $\left\{\phi_m^{f_j^i}\right\}_{m=1}^M$, gives

$$\begin{aligned} &\min_{\mathbf{x}_1,...,\mathbf{x}_M \in \Omega} \textstyle\sum_{m=1}^M \left(\alpha_m^{f_j^i} - \beta_m^{f_j^i}(\mathbf{x}_1,...,\mathbf{x}_M)\right)^2 \\ &\textstyle\sum_{n=1}^M \phi_n^{f_j^i}(\mathbf{x}_m)\beta_n^{f_j^i}(\mathbf{x}_1,...,\mathbf{x}_M) = f_j^i(\mathbf{x}_m), \qquad 1 \le m \le M. \end{aligned} \tag{77}$$

Comparing the optimization problems (77) and (13), the reader may observe that they are identical, with the general function f in (13) replaced by f_j^i, the i^{th} component of $\mathbf{f}_j$, one of the non-linear functions in (64)–(66). Hence, the "best points" algorithm outlined in Section III can be applied to each of these components.

Given a set of interpolation points $\mathbf{x}_m^{f_j^i}$ for f_j^i, the cardinal functions $\psi_m^{f_j^i}$ for f_j^i are defined by

$$\boldsymbol{\phi}_M^{f_j^i}(\mathbf{x}) = \mathbf{A}^{f_j^i} \boldsymbol{\psi}_M^{f_j^i}(\mathbf{x}), \tag{78}$$

where $\boldsymbol{\phi}_M^{f_j^i}(\mathbf{x}) = \left(\phi_1^{f_j^i}(\mathbf{x}),...,\phi_M^{f_j^i}(\mathbf{x})\right)^T$ and $\boldsymbol{\psi}_M^{f_j^i}(\mathbf{x}) = \left(\psi_1^{f_j^i}(\mathbf{x}),...,\psi_M^{f_j^i}(\mathbf{x})\right)^T$, and $A_{mn}^{f_j^i} = \phi_n^{f_j^i}\left(\mathbf{x}_m^{f_j^i}\right)$, for $m,n = 1,...,M$. As before, the (scalar) cardinal functions $\psi_m^{f_j^i}$ satisfy $\psi_m^{f_j^i}\left(\mathbf{x}_n^{f_j^i}\right) = \delta_{mn}$. Given the interpolation points $\left\{\mathbf{x}_m^{f_j^i}\right\}_{m=1}^M$ and cardinal functions $\left\{\psi_m^{f_j^i}\right\}_{m=1}^M$ (78), the i^{th} component ($i = 1,...,5$) of $\mathbf{f}_j$ (64) – (66) is approximated by

$$[f_0^i(\mathbf{V})]_n \approx [[f_0^i]_M(\mathbf{V})]_n = \sum_{m=1}^M [f_0^i]_n \left(\mathbf{V}\left(\mathbf{x}_m^{[f_0^i]_n}\right)\right) \psi_m^{[f_0^i]_n} \in \mathbb{R}, \qquad i = 1,...,5, n = 1,...,M, \tag{79}$$

$$f_j^i(\mathbf{V}) \approx [f_j^i]_M(\mathbf{V}) = \sum_{m=1}^M f_j^i\left(\mathbf{V}\left(\mathbf{x}_m^{f_j^i}\right)\right) \psi_m^{f_j^i} \in \mathbb{R}, \qquad i = 1,..,5, j = 1,...,4. \tag{80}$$

As shown in Section III for a scalar-valued non-linear function f, the projection of each of the $\mathbf{f}_j$ onto the m^{th} reduced basis mode $\boldsymbol{\phi}_m$ can be written as a matrix-vector product. Consider first specifically $\mathbf{f}_1$ (65). Letting ϕ_m^i denote the i^{th}

component of $\boldsymbol{\phi}_m$ for $i = 1,...,5$,

$$\begin{aligned}(\boldsymbol{\phi}_m, [\mathbf{f}_1]_M(\mathbf{V})) &= \textstyle\sum_{i=1}^{5} \left(\phi_m^i, [f_1^i]_M(\mathbf{V})\right) \\ &= \textstyle\sum_{i=1}^{5} \left(\phi_m^i, \sum_{l=1}^{M} f_1^i \left(\sum_{n=1}^{M} a_n(t)\boldsymbol{\phi}_n\left(\mathbf{x}_l^{f_1^i}\right)\right)\psi_l^{f_1^i}\right) \\ &= \textstyle\sum_{i=1}^{5} \int_\Omega \phi_m^i \left[\sum_{l=1}^{M} \left\{ f_1^i \left(\sum_{n=1}^{M} a_n(t)\boldsymbol{\phi}_n\left(\mathbf{x}_l^{f_1^i}\right)\right)\right\}\psi_l^{f_1^i}\right] d\Omega \\ &= \sum_{l=1}^{M} \underbrace{\left[\int_\Omega \left(\phi_m^1\psi_l^{f_1^1}, \phi_m^2\psi_l^{f_1^2}, \phi_m^3\psi_l^{f_1^3}, \phi_m^4\psi_l^{f_1^4}, \phi_m^5\psi_l^{f_1^5}\right) d\Omega\right]}_{\in\mathbb{R}^{1\times 5}} \underbrace{\mathbf{f}_1\left(\sum_{n=1}^{M} a_n(t)\boldsymbol{\phi}_n(\mathbf{x}_m^{\mathbf{f}_1})\right)}_{\in\mathbb{R}^{5\times 1}},\end{aligned} \tag{81}$$

where

$$\mathbf{f}_1\left(\sum_{n=1}^{N} a_n(t)\boldsymbol{\phi}_n(\mathbf{x}_m^{\mathbf{f}_1})\right) \equiv \begin{pmatrix} f_j^1\left(\sum_{n=1}^{m} a_n(t)\boldsymbol{\phi}_n(\mathbf{x}_m^{f_1^1})\right) \\ f_1^2\left(\sum_{n=1}^{M} a_n(t)\boldsymbol{\phi}_n(\mathbf{x}_m^{f_1^2})\right) \\ f_1^3\left(\sum_{n=1}^{M} a_n(t)\boldsymbol{\phi}_n(\mathbf{x}_m^{f_1^3})\right) \\ f_1^4\left(\sum_{n=1}^{M} a_n(t)\boldsymbol{\phi}_n(\mathbf{x}_m^{f_1^4})\right) \\ f_1^5\left(\sum_{n=1}^{m} a_n(t)\boldsymbol{\phi}_n(\mathbf{x}_m^{f_1^5})\right) \end{pmatrix} \in \mathbb{R}^5, \tag{82}$$

(and similarly for $\mathbf{f}_j$, $j = 0,2,...,4$). (81) is a matrix-vector product of the form $\mathbf{G}^{\mathbf{f}_1}\mathbf{f}_1(\mathbf{D}^{\mathbf{f}_1}\mathbf{a}_M)$ where for $l,m = 1,...,M$,

$$\mathbf{G}^{\mathbf{f}_1}_{l,[5(m-1)+1:5m]} = \int_\Omega (\phi_l^1\psi_m^{f_1^1}, \phi_l^2\psi_m^{f_1^2}, \phi_l^3\psi_m^{f_1^3}, \phi_l^4\psi_m^{f_1^4}, \phi_l^5\psi_m^{f_1^5}) d\Omega \in \mathbb{R}^{1\times 5}, \tag{83}$$

By analogy,

$$\mathbf{G}^{\mathbf{f}_{i+1}}_{l,[5(m-1)+1:5m]} = \int_\Omega (\phi_{l,i}^1\psi_m^{f_{i+1}^1}, \phi_{l,i}^2\psi_m^{f_{i+1}^2}, \phi_{l,i}^3\psi_m^{f_{i+1}^3}, \phi_{l,i}^4\psi_m^{f_{i+1}^4}, \phi_{l,i}^5\psi_m^{f_{i+1}^5}) d\Omega \in \mathbb{R}^{1\times 5}, \tag{84}$$

for $i = 1,2,3$. The size of the matrices $\mathbf{G}^{\mathbf{f}_i}$ (83) and (84) are $M \times 5M$. The matrix $\mathbf{D}^{\mathbf{f}_j}$ is defined by

$$\mathbf{D}^{\mathbf{f}_j} \equiv \begin{pmatrix} \boldsymbol{\phi}_1\left(\mathbf{x}_1^{\mathbf{f}_j}\right) & \cdots & \boldsymbol{\phi}_M\left(\mathbf{x}_1^{\mathbf{f}_j}\right) \\ \vdots & \ddots & \vdots \\ \boldsymbol{\phi}_1\left(\mathbf{x}_M^{\mathbf{f}_j}\right) & \cdots & \boldsymbol{\phi}_M\left(\mathbf{x}_M^{\mathbf{f}_j}\right) \end{pmatrix} \in \mathbb{R}^{5M\times M}, \tag{85}$$

for $j = 1,...,4$, with

$$\boldsymbol{\phi}_m\left(\mathbf{x}_n^{\mathbf{f}_j}\right) \equiv \begin{pmatrix} \phi_m^1\left(\mathbf{x}_n^{f_j^1}\right) \\ \phi_m^2\left(\mathbf{x}_n^{f_j^2}\right) \\ \phi_m^3\left(\mathbf{x}_n^{f_j^3}\right) \\ \phi_m^4\left(\mathbf{x}_n^{f_j^4}\right) \\ \phi_m^5\left(\mathbf{x}_n^{f_j^5}\right) \end{pmatrix} \in \mathbb{R}^5, \qquad 1 \le m,n \le M. \tag{86}$$

Similarly, turning one's attention to the left hand side of (68):

$$\begin{aligned}
\textstyle\sum_{k=1}^{M}(\boldsymbol{\phi}_l,[\mathbf{f}_0(\mathbf{V})]_k)\dot{a}_k &= \textstyle\sum_{i=1}^{5}\sum_{k=1}^{M}\left(\phi_l^i,[f_0^i(\mathbf{V})]_k\right)\dot{a}_k \\
&= \textstyle\sum_{i=1}^{5}\sum_{k=1}^{M}\left(\phi_l^i,\sum_{m=1}^{M}\left[f_0^i\left(\sum_{n=1}^{M}a_n(t)\boldsymbol{\phi}_n\left(\mathbf{x}_m^{[f_0^i]_k}\right)\right)\right]_k\psi_m^{[f_0^i]_k}\right)\dot{a}_k \\
&= \textstyle\sum_{i=1}^{5}\sum_{k=1}^{M}\dot{a}_k\int_\Omega\phi_l^i\left\{\sum_{m=1}^{M}\left[f_0^i\left(\sum_{n=1}^{M}a_n(t)\boldsymbol{\phi}_n\left(\mathbf{x}_m^{[f_0^i]_k}\right)\right)\right]_k\psi_m^{[f_0^i]_k}\right\}d\Omega \\
&= \textstyle\sum_{k=1}^{M}\left\{\sum_{m=1}^{M}\underbrace{\left[\int_\Omega(\phi_l^1\psi_m^{[f_0^1]_k},\phi_l^2\psi_m^{[f_0^2]_k},\phi_l^3\psi_m^{[f_0^3]_k},\phi_l^4\psi_m^{[f_0^4]_k},\phi_l^5\psi_m^{[f_0^5]_k})d\Omega\right]}_{\in\mathbb{R}^{1\times5}}\cdot\right. \\
&\qquad\left.\underbrace{\left[\mathbf{f}_0\left(\sum_{n=1}^{M}a_n(t)\boldsymbol{\phi}_n(\mathbf{x}_m^{[\mathbf{f}_0]_k})\right)\right]_k}_{\in\mathbb{R}^{5\times1}}\right\}\dot{a}_k.
\end{aligned}\tag{87}$$

It follows from (87) that the columns of the mass matrix are given by

$$\mathbf{M}_{[1:M],k}=\mathbf{G}^{[\mathbf{f}_0]_k}[\mathbf{f}_0]_k\left(\mathbf{D}^{[\mathbf{f}_0]_k}\mathbf{a}_M\right)\in\mathbb{R}^M,\tag{88}$$

for $k=1,...,M$, where $\mathbf{G}^{[\mathbf{f}_0]_k}$ and $\mathbf{D}^{[\mathbf{f}_0]_k}$ are defined analogously to (83) and (85) respectively.

It follows that, with interpolation the semi-discrete ROM ODE system for the compressible Navier-Stokes equations is not (63), but rather

$$\mathbf{M}\dot{\mathbf{a}}_M+\sum_{i=1}^{4}\mathbf{G}^{\mathbf{f}_i}\mathbf{f}_i(\mathbf{D}^{\mathbf{f}_i}\mathbf{a}_M)=\mathbf{0}.\tag{89}$$

2. Implementation

Once it is constructed, (89) is advanced forward in time using a time-integration scheme, or a time-integration scheme and Newton's method, if the selected time-integration scheme is implicit. The following remarks regarding the implementation of the model reduction procedure developed above are noteworthy.

- In the ROM ODE system *with* interpolation (89), all the inner-products are contained in the $\mathbf{G}^{\mathbf{f}_j}$ matrices (83), which can be pre-computed prior to time integration of the ROM ODE system (89). Similarly, the interpolated mass matrix (88) can also be pre-computed prior to the time-integration of the ROM system.
- With interpolation, the re-computation of inner products involving the non-linear functions and the reduced basis modes at each time step is replaced by the evaluation of the non-linear functions (82) at a set of M pre-selected interpolation points. In general, $M<<N$, where N is the number of spatial discretization points.
- In a numerical implementation, for the sake of computing the required continuous L^2 inner products involving the POD modes and their derivatives, the reduced basis (e.g., a POD basis) are described by a finite element representation of the computational mesh. The required inner products are then computed using a Gauss quadrature rule.[1–3,13] This approach is fairly general, as long as the simulation code can output data to a nodal mesh and the mesh can be cast as a collection of finite elements.
- The "best" interpolation points appearing in (86) are computed in the offline stage of the model reduction procedure, for each of the components of the non-linear functions that appear in (83). For a detailed discussion of the computational complexity of the "best points" interpolation algorithm, the reader is referred to Peraire, Nguyen *et al.*[16,17] Although the offline construction of the proposed reduced order model is computationally intensive, this computation is performed only once, and would not inhibit any online real-time predictive computations that the model may be needed for.[16,17]
- The time-integration of the ROM ODE system (89) requires the factorization of the matrix $\mathbf{M}$, an $M\times M$ dense matrix. However, since the number of modes M will in general be quite small, this matrix will be quite small.

VI. Preliminary Numerical Studies: Scalar Conservation Laws

This section presents some preliminary results for the model reduction procedure proposed above. The procedure is applied to some non-linear scalar conservation laws of the form

$$u_{,t} + [f(u)]_{,x} = \mu u_{,xx}, \tag{90}$$

where $f(u)$ is the flux function. (90) is a simpler scalar non-linear model for the Navier-Stokes equations (22). The degree of non-linearity in (90) depends on the flux function $f(u)$. The primary objective of these preliminary numerical studies is to gauge the viability of the Proper Orthogonal Decomposition (POD)/Galerkin method for model reduction outlined above, both without as well as with interpolation, when applied to non-linear conservation laws whose solution possess inherently non-linear features in common with features of solutions to the compressible Navier-Stokes equations (22), such as shocks and rarefactions.

A. Entropy Stability and Scalar Conservation Laws

Before proceeding to the numerical studies, some discussion of entropy stability in the context of conservation laws of the form (90) is in order, so as to connect the present section to the first part of this paper. It is well known that the differential equation (90) is not valid in the classical sense for solutions containing shocks (discontinuities). This motivates one to seek so-called weak solutions to these equations. In general, weak solutions to (90) are non-unique. In developing a numerical method for (90) it is crucial that the selected method computes a weak solution to this law that is physically correct, or "admissible". As for the Navier-Stokes equations, "admissibility conditions" are closely tied to the concept of entropy – indeed, they are often referred to as "entropy conditions". These conditions demand that the entropy across a shock should increase. Mathematically, this requirement results in a range of admissible speeds at which the discontinuity or shock is allowed to propagate (the well known Rankine-Hugoniot and Oleinik entropy conditions, for convex and non-convex flux functions $f(u)$ respectively).

For *scalar* conservation laws of the form (90) such as the two examples considered here, it can be shown[34,35] that

$$H = \frac{1}{2}u^2, \tag{91}$$

defines a valid generalized entropy function. It follows that $v = u$ (35), that is, no transformation is required to ensure *a priori* entropy stability of the Galerkin projection step of the model reduction procedure.

Remark 3: Note that the generalized entropy function is such that the transformation (35) is non-trivial for *systems* of conservation laws of the form:

$$\mathbf{u}_{,t} + \nabla \mathbf{f}(\mathbf{u}) = \mathbf{0}, \tag{92}$$

such as, for example, the shallow water equations and the equations of gas dynamics.[5,8,12,34,42] Although the examples below are for scalar equations, the extension to non-linear systems is straightforward.[36]

For both test problems considered in this section, the reduced basis employed was a POD basis, obtained in the usual L^2 inner product from snapshots of "high-fidelity" solutions computed using a third order ENO-LLF method[34] in space and fourth order Runge-Kutta method in time.

B. Burgers' Equation

Consider the following initial boundary value problem (IBVP) for Burgers' equation, a scalar conservation law of the form (90) with quadratic flux function $f(u) = \frac{1}{2}u^2$.

$$\begin{aligned} &u_t + \left(\tfrac{u^2}{2}\right)_x = \mu u_{xx}, \qquad -1 < x < 3, \quad 0 < t < T, \\ &u(-1,t) = u(3,t) = 0, \qquad\qquad\qquad\quad 0 < t < T, \end{aligned} \tag{93}$$

with initial condition

$$u(x,0) = \begin{cases} 0, & x < 0, \\ 1, & 0 \le x < 1, \\ 0, & x \ge 1. \end{cases} \tag{94}$$

Discontinuous initial data (94) are specified such that both a rarefaction and a shock form in the $\mu \to 0$ limit. A total of $K = 101$ snapshots of this solution were taken, at increments $\Delta t_{snap} = 0.03$, up to time $T = 3$, computed with spatial mesh increment $\Delta x = 0.008$.

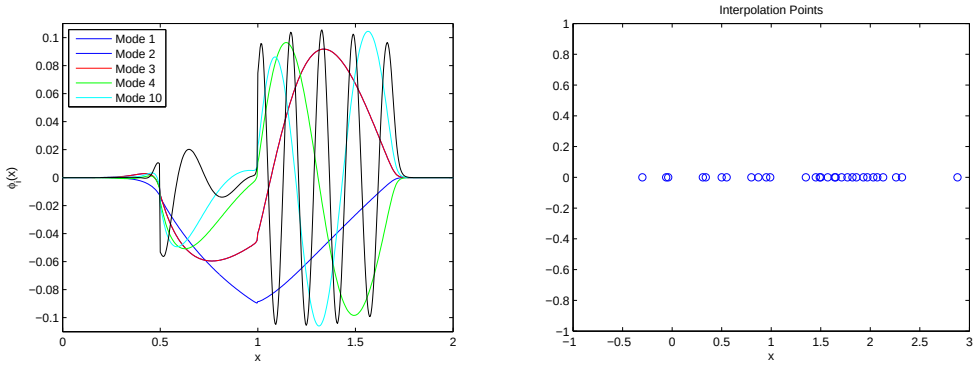

(a) POD modes

(b) Interpolation Points x^{bp} $(M = 30)$

Figure 1. POD modes and interpolation points for the Burgers' IBVP (93)

The POD modes for this problem are shown in Figure 1 (a). The reader may remark that higher order modes are oscillatory in nature. The reader may also observe that the POD modes are not $C^1(\Omega)$. This is not surprising, as the snapshots from which the POD modes were computed were not even $C^0(\Omega)$. In the discrete implementation of the ROM, care must be taken to ensure that the derivatives that appear in the weak form of the problem are well-defined locally for the purpose of evaluating the required inner products.

The interpolation points computed via the BPIM method of Peraire, Nguyen *et al.*[16,17] and outlined in Section III are shown in Figure 1 (b). The spacing of the points is reasonable given the character of the exact solution to this problem (Figure 2).

Figures 2–3 show the computed ROM solution using a POD basis with $M = 30$ modes without and with the "best points" interpolation respectively. The ROMs are able to capture the essential features of the solution, namely the weak shock and rarefaction. Minor oscillations are apparent in the vicinity of the weak shock. This suggests that the addition of some artificial viscosity may be required[4,18] when μ is small to capture accurately the shock (Section III.C.3).

C. Buckley-Leverett Equation

The other conservation law considered is the so-called Buckley-Leverett equation, which has a highly non-linear, non-convex flux $f(u) = \frac{u^2}{u^2+(1-u)^2}$:

$$\begin{aligned} &u_t + \left(\frac{u^2}{u^2+(1-u)^2}\right)_x = \mu u_{xx}, \quad -1.5 < x < 1.5, \quad 0 < t < T, \\ &u(-1.5,t) = u(1.5,t) = 0, \qquad\qquad\qquad\quad 0 < t < T, \\ &u(x,0) = e^{-16x^2}, \qquad\qquad -1.5 < x < 1.5. \end{aligned} \tag{95}$$

The equation is sometimes used to model two-phase flow in porous media. A 2D variant of this problem has been considered by other authors in the context of model order reduction.[16,17] To build the POD basis, $K = 50$ snapshots were taken from the high-fidelity, with temporal spacing $\Delta t_{snap} = 0.0102$, and a spatial mesh increment $\Delta x = 0.0151$.

Figure 4 (a) shows the first four and the last POD mode for this problem. The initial condition for this problem is $C^\infty(\Omega)$ and the solutions possesses only a weak shock, so the POD modes are more smooth than the POD modes for the problem in Section VI.B (Figure 1 (a)). As for the problem in Section VI.B, higher order modes are oscillatory in nature.

The "best points" are shown in Figure 4 (b). Given the strong non-linearity in the flux $f(u)$, the BPIM greatly improves complexity for this problem.

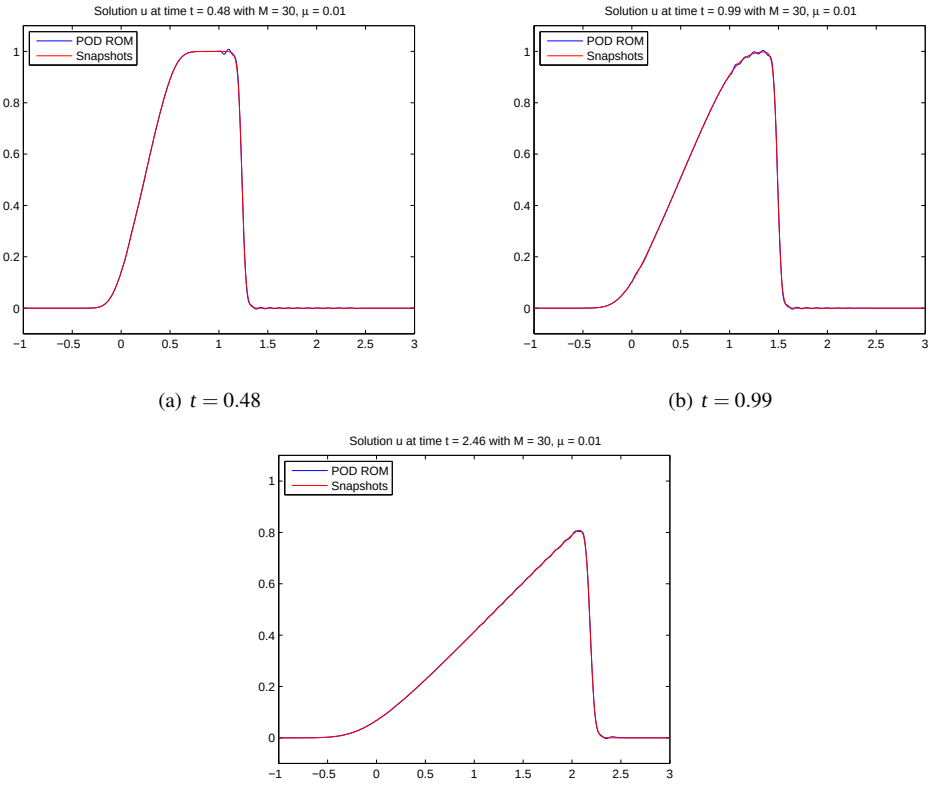

(a) $t = 0.48$

(b) $t = 0.99$

(c) $t = 2.46$

Figure 2. POD ROM solution to the Burgers' IBVP (93) **with** $M = 30$ **(no interpolation)**

Results for POD ROMs with $M = 10$ modes without and with interpolation respectively are shown in Figures 5–6 respectively. The ROMs perform equally well: the ROM solution with interpolation (Figure 5) is indistinguishable from the ROM solution without interpolation (Figure 6).

VII. Conclusions and Future Work

This paper presents techniques for building entropy stable and efficient reduced order models (ROMs) governed by non-linear partial differential equations (PDEs) in fluid mechanics, namely the full compressible Navier-Stokes equations. In effect, the techniques are a natural extension of the stability-preserving model reduction methodology developed in earlier work[1–3,13] specifically for the *linearized* compressible flow equations. The non-linearity present in the full compressible flow equations presents a challenge for developing provably stable and efficient ROMs. The challenge of stability is addressed with the help of a transformation that effectively symmetrizes these equations. It is proven that the Galerkin projection of the equations gives rise to a discrete model that obeys an essential property of the governing equations, namely the second law of thermodynamics, or Clausius-Duhem inequality. The practical implication of this result is that if the ROM is built in the so-called "entropy variables", entropy stability is guaranteed *a priori* for *any* choice of reduced basis. It is shown that the online computational complexity of the ROM can be reduced by handling the non-linearities present in the governing equations efficiently using the "best points" interpolation method.[16,17] Preliminary numerical tests on some scalar conservation laws whose solutions possess features akin to the solutions of the compressible Navier-Stokes equations suggest that the model reduction procedure with a proper orthogonal decomposition (POD) basis and the "best points" interpolation can capture accurately and efficiently non-linear phenomena such as rarefactions and shocks. These tests also reinforce the conjecture that the addition of stabilization and/or shock-capturing terms to the variational formulation may be required in the presense of sharp layers and/or strong shocks.

Future work will involve implementing the reduced order model formulated in the present work and evaluating its

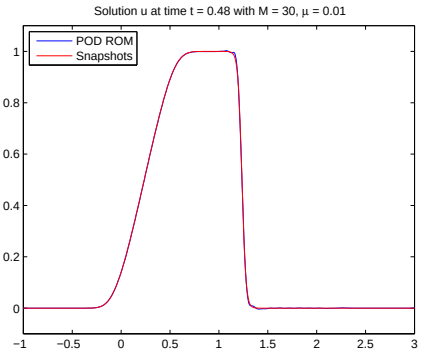

(a) $t = 0.48$

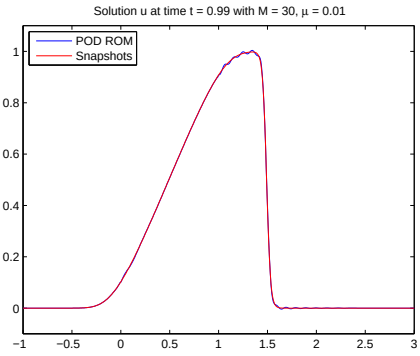

(b) $t = 0.99$

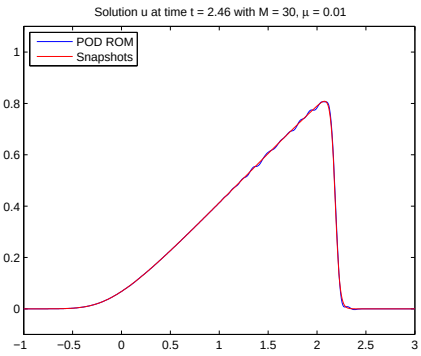

(c) $t = 2.46$

Figure 3. POD ROM solution to the Burgers' IBVP (93) **with** $M = 30$ **(with the "best points" interpolation)**

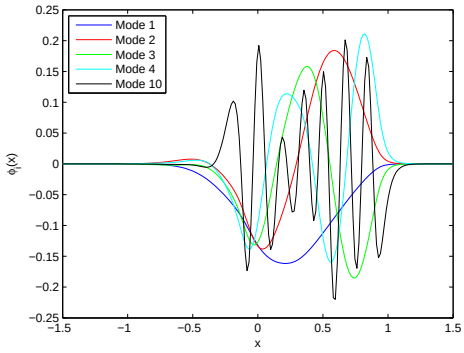

(a) POD modes

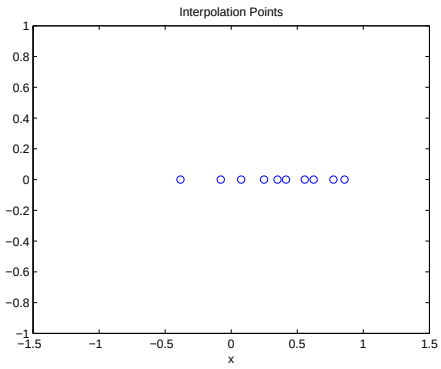

(b) x^{bp} $(M = 10)$

Figure 4. POD modes and interpolation points for the Buckley-Leverett IBVP (95)

performance on benchmark problems of relevance in the field of aeronautics. Since the theoretical results established in this paper are basis-independent, the use of alternate bases (e.g., balanced POD) to represent the solution will be examined. Robustness with respect to parameter changes will be explored using recent developments in the area of reduced basis interpolation.[32] Techniques for incorporation of turbulence models, as well as stabilization and shock capturing operators, into the ROM formulation will be derived.

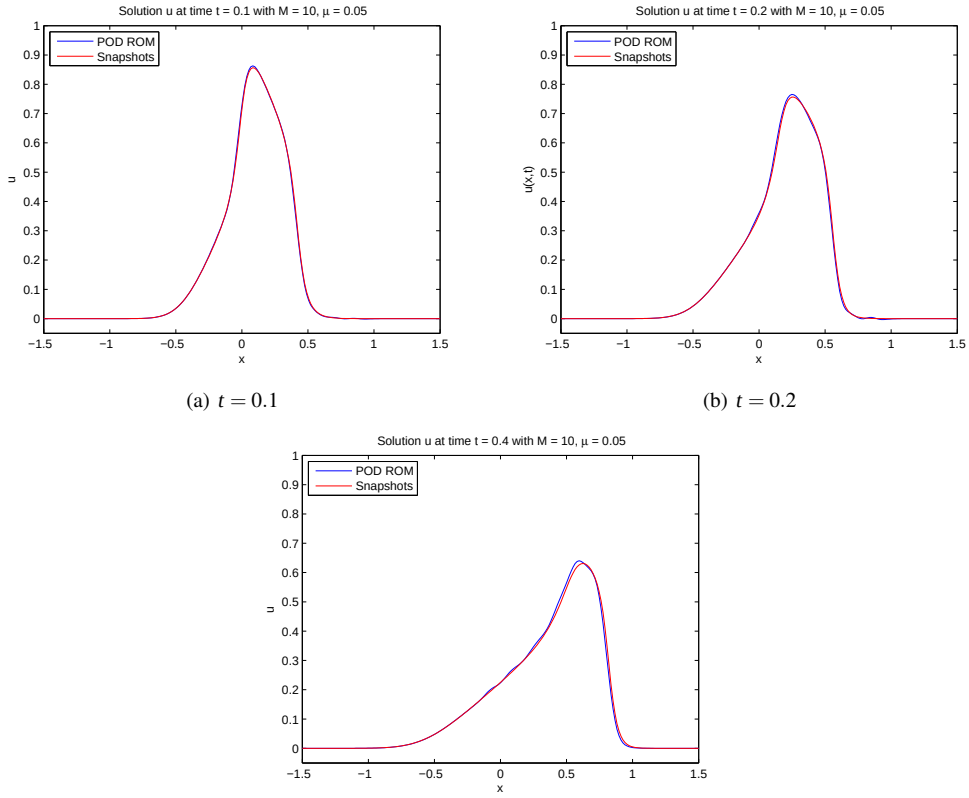

(a) $t = 0.1$

(b) $t = 0.2$

(c) $t = 0.4$

Figure 5. POD ROM solution to Buckley-Leverett IBVP (95) **with** $M = 10$ **(no interpolation)**

Appendix: Compressible Navier-Stokes System Matrices and Vectors in the Entropy Variables

To simplify the notation, the following variables are introduced[c]:

$$\begin{array}{lll} \bar{\gamma} = \gamma - 1, & k_1 = \frac{1}{2V_5}(V_2^2 + V_3^2 + V_4^2), & k_2 = k_1 - \gamma, \\ k_3 = k_1^2 - 2\gamma k_1 + \gamma, & k_4 = k_2 - \bar{\gamma}, & k_5 = k_2^2 - \bar{\gamma}(k_1 + k_2), \\ c_1 = \bar{\gamma}V_5 - V_2^2, & d_1 = -V_2V_3, & e_1 = V_2V_5, \\ c_2 = \bar{\gamma}V_5 - V_3^2, & d_2 = -V_2V_4, & e_2 = V_3V_5, \\ c_3 = \bar{\gamma}V_5 - V_4^2, & d_3 = -V_3V_4, & e_3 = V_4V_5. \end{array} \tag{96}$$

In the entropy variables $\mathbf{V}$, the Euler fluxes $\tilde{\mathbf{F}}_i(\mathbf{V})$ are given by:

$$\tilde{\mathbf{F}}_1(\mathbf{V}) = \frac{\rho_1}{V_5}\begin{pmatrix} e_1 \\ c_1 \\ d_1 \\ d_2 \\ k_2V_2 \end{pmatrix}, \quad \tilde{\mathbf{F}}_2(\mathbf{V}) = \frac{\rho_1}{V_5}\begin{pmatrix} e_2 \\ d_1 \\ c_2 \\ d_3 \\ k_2V_3 \end{pmatrix}, \quad \tilde{\mathbf{F}}_3(\mathbf{V}) = \frac{\rho_1}{V_5}\begin{pmatrix} e_3 \\ d_2 \\ d_3 \\ c_3 \\ k_2V_4 \end{pmatrix}. \tag{97}$$

[c]This section is repeated here from the Appendix of Hughes *et al.*[12] to make this document self-contained.

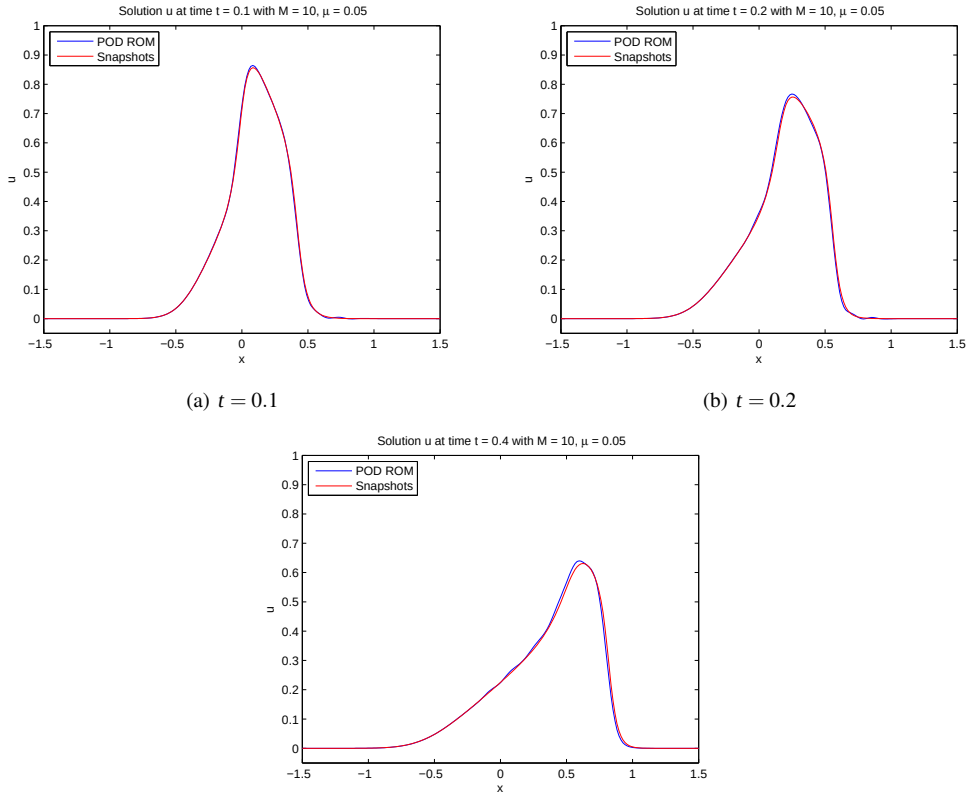

(a) $t = 0.1$

(b) $t = 0.2$

(c) $t = 0.4$

Figure 6. POD ROM solution to Buckley-Leverett IBVP (95) **with** $M = 10$ **(with the "best points" interpolation)**

The symmetrizing matrix $\mathbf{A}_0$ and its inverse are given by

$$\mathbf{A}_0 = \mathbf{U}_{,\mathbf{V}} = \frac{\rho_1}{\bar{\gamma} V_5} \begin{pmatrix} -V_5^2 & e_1 & e_2 & e_3 & V_5(1-k_1) \\ & c_1 & d_1 & d_2 & V_2 k_2 \\ & & c_2 & d_3 & V_3 k_2 \\ & & & c_3 & V_4 k_2 \\ \text{symm.} & & & & -k_3 \end{pmatrix}, \tag{98}$$

and

$$\mathbf{A}_0^{-1} = \mathbf{V}_{,\mathbf{U}} = -\frac{1}{\rho_1 V_5} \begin{pmatrix} k_1^2+\gamma & k_1 V_2 & k_1 V_3 & k_1 V_4 & (k_1+1)V_5 \\ & V_2^2 - V_5 & -d_1 & -d_2 & e_1 \\ & & V_3^2 - V_5 & -d_3 & e_2 \\ & & & V_4^2 - V_5 & e_3 \\ \text{symm.} & & & & V_5^2 \end{pmatrix}. \tag{99}$$

Here,

$$\rho_1 = \left[\frac{\gamma - 1}{(-V_5)^\gamma}\right]^{1/(\gamma-1)} \exp\left(\frac{-s}{\gamma-1}\right). \tag{100}$$

The Jacobians of the Euler fluxes are:

$$\tilde{\mathbf{A}}_1 = \mathbf{F}_{1,\mathbf{V}} = \frac{\rho_1}{\bar{\gamma} V_5^2} \begin{pmatrix} e_1 V_5 & c_1 V_5 & d_1 V_5 & d_2 V_5 & k_2 e_1 \\ & -(c_1 + 2\bar{\gamma} V_5) V_2 & -c_1 V_3 & -c_1 V_4 & c_1 k_2 + \bar{\gamma} V_2^2 \\ & & -c_2 V_2 & -d_1 V_4 & k_4 d_1 \\ & & & -c_3 V_2 & k_4 d_2 \\ \text{symm.} & & & & k_5 V_2 \end{pmatrix}, \tag{101}$$

$$\tilde{\mathbf{A}}_2 = \mathbf{F}_{2,\mathbf{V}} = \frac{\rho_1}{\bar{\gamma} V_5^2} \begin{pmatrix} e_2 V_5 & d_1 V_5 & c_2 V_5 & d_3 V_5 & k_2 e_2 \\ & -c_1 V_3 & -c_2 V_2 & -d_1 V_4 & k_4 d_1 \\ & & -(c_2 + 2\bar{\gamma} V_5) V_3 & -c_2 V_4 & c_2 k_2 + \bar{\gamma} V_3^2 \\ & & & -c_3 V_3 & k_4 d_3 \\ \text{symm.} & & & & k_5 V_3 \end{pmatrix}, \tag{102}$$

$$\tilde{\mathbf{A}}_3 = \mathbf{F}_{3,\mathbf{V}} = \frac{\rho_1}{\bar{\gamma} V_5^2} \begin{pmatrix} e_3 V_5 & d_2 V_5 7 d_3 V_5 & c_3 V_5 & k_2 e_3 & \\ & -c_1 V_4 & -d_2 V_3 & -c_3 V_2 & k_4 d_2 \\ & & -c_2 V_4 & -c_3 V_3 & k_4 d_3 \\ & & & -(c_3 + 2\bar{\gamma} V_5) V_4 & c_3 k_2 + \bar{\gamma} V_4^2 \\ \text{symm.} & & & & k_5 V_4 \end{pmatrix}. \tag{103}$$

The velocity and temperature can be written in the entropy variables as:

$$u_i(\mathbf{V}) = -\frac{V_{i+1}}{V_5}, \quad i = 1, 2, 3, \tag{104}$$

$$\theta(\mathbf{V}) = -\frac{1}{c_v V_5}, \tag{105}$$

The gradients of the viscous and heat fluxes are given by:

$$u_{i,j} = \frac{-V_5 V_{i+1,j} + V_{i+1} V_{5,j}}{V_5^2}, \tag{106}$$

$$\kappa \theta_{,i} = \frac{\gamma \mu}{Pr} \frac{1}{V_5^2} V_{5,i}, \tag{107}$$

where $Pr \equiv \mu c_p / \kappa$ is the Prandtl number.

Finally, the symmetrized viscous and heat flux matrices $\tilde{\mathbf{K}}_{ij} \equiv \tilde{\mathbf{K}}_{ij}^v + \tilde{\mathbf{K}}_{ij}^h$ are given by:

$$\tilde{\mathbf{K}}_{11} = \frac{1}{V_5^3} \begin{pmatrix} 0 & 0 & 0 & 0 & 0 \\ 0 & -(\gamma - 2\mu) V_5^2 & 0 & 0 & (\lambda + 2\mu) e_1 \\ 0 & 0 & -\mu V_5^2 & 0 & \mu e_2 \\ 0 & 0 & 0 & -\mu V_5^2 & \mu e_3 \\ 0 & (\lambda + 2\mu) e_1 & \mu e_2 & \mu e_3 & -\left[(\lambda + 2\mu) V_2^2 + \mu (V_3^2 + V_4^2) - \frac{\gamma \mu V_5}{Pr} \right] \end{pmatrix}, \tag{108}$$

$$\tilde{\mathbf{K}}_{12} = \frac{1}{V_5^3} \begin{pmatrix} 0 & 0 & 0 & 0 & 0 \\ 0 & 0 & -\lambda V_5^2 & 0 & \lambda e_2 \\ 0 & -\mu V_5^2 & 0 & 0 & \mu e_1 \\ 0 & 0 & 0 & 0 & 0 \\ 0 & \mu e_2 & \lambda e_1 & 0 & (\lambda + \mu) d_1 \end{pmatrix}, \tag{109}$$

$$\tilde{\mathbf{K}}_{13} = \frac{1}{V_5^3} \begin{pmatrix} 0 & 0 & 0 & 0 & 0 \\ 0 & 0 & 0 & -\lambda V_5^2 & \lambda e_3 \\ 0 & 0 & 0 & 0 & 0 \\ 0 & -\mu V_5^2 & 0 & 0 & \mu e_1 \\ 0 & \mu e_3 & 0 & \lambda e_1 & (\lambda + \mu) d_2 \end{pmatrix}, \tag{110}$$

$$\tilde{\mathbf{K}}_{22} = \frac{1}{V_5^3} \begin{pmatrix} 0 & 0 & 0 & 0 & 0 \\ 0 & -\mu V_5^2 & 0 & 0 & \mu e_1 \\ 0 & 0 & -(\lambda + 2\mu) V_5^2 & 0 & (\lambda + 2\mu) e_2 \\ 0 & 0 & 0 & -\mu V_5^2 & \mu e_3 \\ 0 & \mu e_1 & (\lambda + 2\mu) e_2 & \mu e_3 & -\left[(\lambda + 2\mu) V_3^2 + \mu (V_2^2 + V_4^2) - \frac{\gamma \mu V_5}{Pr} \right] \end{pmatrix}, \tag{111}$$

$$\tilde{\mathbf{K}}_{23} = \frac{1}{V_5^3}\begin{pmatrix} 0 & 0 & 0 & 0 & 0 \\ 0 & 0 & 0 & 0 & 0 \\ 0 & 0 & 0 & -\lambda V_5^2 & \lambda e_3 \\ 0 & 0 & -\mu V_5^2 & 0 & \mu e_2 \\ 0 & 0 & \mu e_3 & \lambda e_2 & (\lambda+\mu) d_3 \end{pmatrix}, \tag{112}$$

$$\tilde{\mathbf{K}}_{33} = \frac{1}{V_5^3}\begin{pmatrix} 0 & 0 & 0 & 0 & 0 \\ 0 & -\mu V_5^2 & 0 & 0 & \mu e_1 \\ 0 & 0 & -\mu V_5^2 & 0 & \mu e_2 \\ 0 & 0 & 0-(\lambda+2\mu)V_5^2 & (\lambda+2\mu)e_3 & \\ 0 & \mu e_1 & \mu e_2 & (\lambda+2\mu)e_3 & -\left[(\lambda+2\mu)V_4^2+\mu(V_2^2+V_3^2)-\frac{\gamma\mu V_5}{Pr}\right] \end{pmatrix}, \tag{113}$$

with

$$\tilde{\mathbf{K}}_{21} = \tilde{\mathbf{K}}_{12}^T, \quad \tilde{\mathbf{K}}_{31} = \tilde{\mathbf{K}}_{13}^T, \quad \tilde{\mathbf{K}}_{32} = \tilde{\mathbf{K}}_{23}^T. \tag{114}$$

Acknowledgments

This research was funded by Sandia National Laboratories Laboratory Directed Research and Development (LDRD) program. Sandia is a multiprogram laboratory operated by Sandia Corporation, a Lockheed Martin Company for the United States Department of Energy's National Nuclear Security Administration under contract DE-AC04-94AL85000. The first author acknowledges the support of an NDSEG Fellowship sponsored by the U.S. Department of Defense, and also the support of a National Physical Science Consortium (NPSC) Fellowship, funded by the Engineering Sciences Center at Sandia National Laboratories.

References

[1]M. F. Barone, I. Kalashnikova, D.J. Segalman, H.K. Thornquist. Stable Galerkin Reduced Order Models for Linearized Compressible Flow. *J. Comput. Phys.* **228** (2009) 1932–1946.

[2]M.F. Barone, I. Kalashnikova, M.R. Brake, D.J. Segalman. Reduced Order Modeling of Fluid/Structure Interaction. *Sandia National Laboratories Report, SAND No. 2009-7189.* Sandia National Laboratories, Albuquerque, NM (2009).

[3]M.F. Barone, D.J. Segalman, H.K. Thornquist, I. Kalashnikova, Galerkin Reduced Order Models for Compressible Flow with Structural Interaction, *AIAA 46th Aerospace Science Meeting and Exhibit*, AIAA 2008-0612, Reno, NV (2008).

[4]E. Burman. On nonlinear artificial viscosity, discrete maximum principle and hyperbolic conservation laws. *BIT Numer. Math.* **47**:715–733 (2007).

[5]M. Gerritsen, P. Olsson. Designing an Efficient Solution Strategy for Fluid Flows: 1. A Stable High Order Finite Difference Scheme and Sharp Shock Resolution for the Euler Equations. *J. Comput. Phys.* **129**:245–262 (1996).

[6]D. Funaro, D. Gottlieb, Convergence results for Pseudospectral Approximations of Hyperbolic Systems by a Penalty-Type Boundary Treatment, *Math. of Comput.* **57**(196) 585-596 (1991).

[7]J.S. Hesthaven, D. Gottlieb, A Stable Method for the Compressible Navier-Stokes Equations: I. Open Boundary Conditions, *SIAM J. Sci. Comput.*, **17**(3) 579-612 (1996).

[8]A. Harten. On the symmetric form of systems of conservations laws with entropy. *J. Comput. Phys.* **49**: 151–164 (1983).

[9]P. Holmes, J.L. Lumley, G. Berkooz, Turbulence, Coherent Structures, Dynamical Systems and Symmetry, New York, NY: Cambridge University Press, 1996.

[10]L. Sirovich. Turbulence and the dynamics of coherent structures, Part III: Dynamics and scaling. *Quarterly of Applied Mathematics*, **45** (3) 583–590 (1987).

[11]N. Aubry, P. Holmes, J. Lumley, and E. Stone. The dynamics of coherent structures in the wall region of a turbulent boundary layer. *J. Fluid Mech.*, **192** 115–173 (1988).

[12]T.J.R. Hughes, L.P. Franca, M. Mallet. A new finite element formulation for computational fluid dynamics: I. Symmetric forms of the compressible Euler and Navier-Stokes equations and the second law of thermodynamics. *Comput. Meth. Appl. Mech. Engng.* **54**:223–234 (1986).

[13]I. Kalashnikova, M.F. Barone. On the Stability and Convergence of a Galerkin Reduced Order Model (ROM) of Compressible Flow with Solid Wall and Far-Field Boundary Treatment. *Int. J. Numer. Meth. Engng.* **83**:1345–1375 (2010).

[14]K. Kunisch, S. Volkwein, Galerkin Proper Orthogonal Decomposition for a General Equation in Fluid Dynamics, *SIAM J. Numer. Anal.*, **40**(2) 492–515 (2002).

[15]J.L. Lumley, Stochastic Tools in Turbulence. New York, NY: Academic Press, 1971.

[16]N.C. Nguyen, A.T. Patera, J. Peraire. A 'best points' interpolation method for efficient approximation of parametrized functions. *Int. J. Numer. Meth. Engng.* **73**:521–543 (2008).

[17]N.C. Nguyen, J. Peraire. An efficient reduced-order modeling approach for non-linear parametrized partial differential equations. *Int. J. Numer. Meth. Engng.* **76**:27–55 (2008).

[18]T.E. Tezduyar, M. Senga. Stabilization and shock-capturing parameters in SUPG formulation of compressible flows. *Comput. Meth. Appl. Mech. Engrg.* **195**:1621–1632 (2006).

[19]M. Rathinam, L.R. Petzold, L.R. A New Look at Proper Orthogonal Decomposition, *SIAM J. Numer. Anal.* **41** (5) 1893–1925 (2003).

[20]K. Veroy, A.T. Patera. Certified real-time solution of the parametrized steady incompressible Navier-Stokes equations: rigorous reduced-basis a posteriori error bounds. *Int. J. Num.Meth. Fluids*, **47** 773–788 (2005).

[21]K. Willcox, J. Peraire. Balanced model reduction via the proper orthogonal decomposition. *A*IAA J., **40** (11) 2323–2330 (2002).

[22]C.W. Rowley. Model reduction for fluids, using balanced proper orthogonal decomposition. *Int. J. Bifurcation and Chaos*, **15** (3) 997–1013 (2005).

[23]C.W. Rowley, T. Colonius, R.M. Murray. Model reduction for compressible flows using POD and Galerkin projection. *Physica D. Nonlinear Phenomena* **189** (1–2) 115–129 (2004).

[24]K. Carlberg, C. Bou-Mosley, C. Farhat. Efficient non-linear model reduction via a least-squared Petrov-Galerkin projection and compressive tensor approximations. *Int. J. Numer. Meth. Engng.* **86** (2) 155–181 (2011).

[25]R. Everson, L. Sirovich. Karhunen-Loeve procedure for gappy data. *J. Opt. Society of America A.* **12** (8) 1657–1664 (1995).

[26]T. Bui-Thanh, K. Willcox, O. Ghattas, and B. van Bloemen Waanders. Goal-oriented, model-constrained optimization for reduction of large-scale systems. *J. Comp. Phys.*, **224** 880–896 (2007).

[27]J.A. Taylor, M.N. Glauser. Towards practical flow sensing and control via POD and LSE based low-dimensional tools. *J. Fluids Eng.*, **126** (3) 337–345 (2003).

[28]A. LeGresley, J.J. Alonso. Investigation of non-linear projection for POD based reduced order models for aerodynamics. *39th AIAA Aerospace Sciences Meeting & Exhibit*, AIAA Paper 2001-0926 (2001)

[29]K.C. Hall, J.P. Thomas, E.H. Dowell. Proper orthogonal decomposition technique for transonic unsteady aerodynamic flows. *AIAA J.*, **38** (10) (2000).

[30]T. Lieu, C. Farhat, M. Lesoinne. Reduced-order fluid/structure modeling of a complete aircraft configuration. *Comput. Methods Appl. Mech. Engng.*, **195** 5730–5742 (2006).

[31]T. Lieu, C. Farhat. Aerodynamic parameter adaptation of CFD-based reduced-order models. *45th Aerospace Sciences Meeting and Exhibit*, AIAA Paper 2007-328 (2007).

[32]D. Amsallem, C. Farhat. An interpolation method for adapting reduced-order models and application to aeroelasticity. *AIAA J.* **46** (7) 1803–1813 (2008).

[33]D. Amsallem, J. Cortial, K. Carlberg, C. Farhat. A method for interpolating on manifolds structural dynamics reduced-order models. *Int. J. Numer. Meth. Engng.* **80** 1241–1258 (2009).

[34]R.J. LeVeque. Finite Volume Methods for Hyperbolic Problems. Port Chester, NY: Cambridge University Press, 2002.

[35]R. Ansorge. Convergence of Discretizations of Nonlinear Problems: A General Approach. *J. Appl. Math. & Mech.* **73** (10) 239–253 (1993).

[36]I. Kalashnikova, M.F. Barone. Efficient Non-Linear Proper Orthogonal Decompositino (POD)/Galerkin Reduced Order Models with Stable Penalty Enforcement of Boundary Conditions, *under review for publication in Int. J. Numer. Meth. Engng*.

[37]T.J.R. Hughes, M. Mallet. A new finite element formulation for computational fluid dynamics: III. The generalized streamline operator for multidimensional advective-diffusive systems, *Comput. Meth. Appl. Mech. Engng.* **58** 305–328 (1986).

[38]T.J.R. Hughes. Recent progress in the development and understanding of SUPG methods with specicial reference to the compressible Euler and Navier-Stokes equations, *Int. J. Numer. Meth. Fluids.* **7** 1261–1275 (1987).

[39]T.J.R. Hughes, M. Mallet. A new finite element formulation for computational fluid dynamics: IV. A discontinuity-capturing operator for multi-dimensional advective-diffusive systems, *Comput. Meth. Appl. Mech. Engng.* **58** 329–336 (1986).

[40]F. Shakib, T.J.R. Hughes, Z. Johan. A new finite element formulation for computational fluid dynamics: X. The compressible Euler and Navier-Stokes equations, *Comput. Meth. Appl. Mech. Engng.* **89** 141–219 (1991).

[41]F. Chalot, T.J.R. Hughes, F. Shakib. Symmetrization of conservation laws with entropy for high-temperature hypersonic computations, *Comput. Sys. Engng.* **1** (2–4) 495–521 (1990).

[42]S.W. Bova, G.F. Carey. An entropy variable formulation and applications for the two-dimensional shallow water equations, *Int. J. Numer. Meth. Fluids* **23** 29–46 (1996).